05D2008 MD. Rafiquzzaman

Strength of material laboratory, Dept. of Mechanical Engineering, Saitama University, Japan

Date: 7th February, 2008

Fracture mechanism of an aluminium cast alloy locally reinforced by SiC particles and Al_2O_3 whiskers under monotonic and cyclic load: stress distribution and whisker orientation effect.

一部分がSiC粒子とAl_2O_3ウィスカで強化されたAl鋳造合金の単調および繰返し荷重下における破壊機構の評価：応力分布およびウィスカー方向の効果

Presentation outline

1. Introduction

2. Part-1: Fracture mechanism and stress distribution under monotonic and cyclic load

3. Part-2: Effect of whisker orientation on monotonic and fatigue strength

4. Conclusions

1. Introduction

1.1. Background

1.2. Applications of MMCs

1.3. Concept of locally reinforced material

1.4. Review of the researchers

1.5. Motivation of current research

1.6. Scope and objectives

1.1 Background

Mechanical component

Made by

Traditional Material

(Plastics, metals, ceramics etc)

Under service condition

Not give all properties

Promising Solution

Metal Matrix Composites (MMCs)

1.1 Background

- **Metal matrix composite (MMC) that contains two or more discrete insoluble phases**

- **Typical benefits:**
  - **High strength and stiffness**
  - **Light weight or low density**
  - **Higher modulus**
  - **Higher wear resistance**

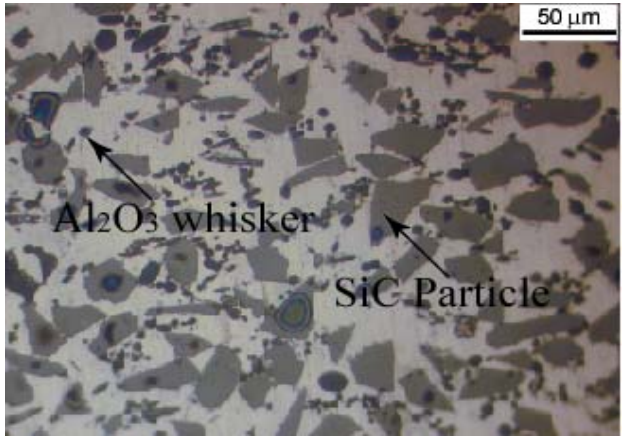

AC4CH alloy, 21vol.% SiC particles and 9 vol.% Al_2O_3whiskers (hybrid MMC)

1.2 Application of MMCs

Major applications

Automotive Industries:

- Engine blokes, intake and exhaust valves
- Driveshaft and propshafts
- Brake component (Discs, rotor, calipers)
- Piston rod
- Cylinder bores

Applications in aerospace:

- Ventral fins
- Fuel access door cover
- Rotor blades

Others applications:

- Golf club shaft and head
- Skating shoe
- Base ball shaft

1.3 Concept of locally reinforced material

A carrier body which consist partially reinforced cast part called locally reinforced material.

Example:

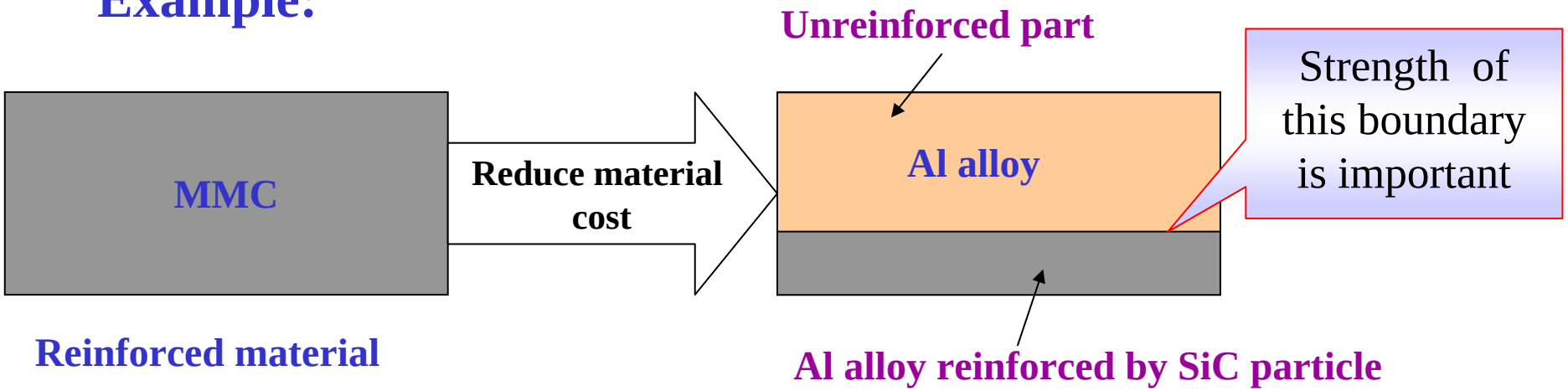

1.3 Concept of locally reinforced material

MMC

Mechanically superior

Low ductility

High price

Locally reinforced material

Mechanically superior
+
Cost effective

MMC with a ductile carrier body

Confine the application of the MMC to the most important frictional area

1.3 Concept of locally reinforced material

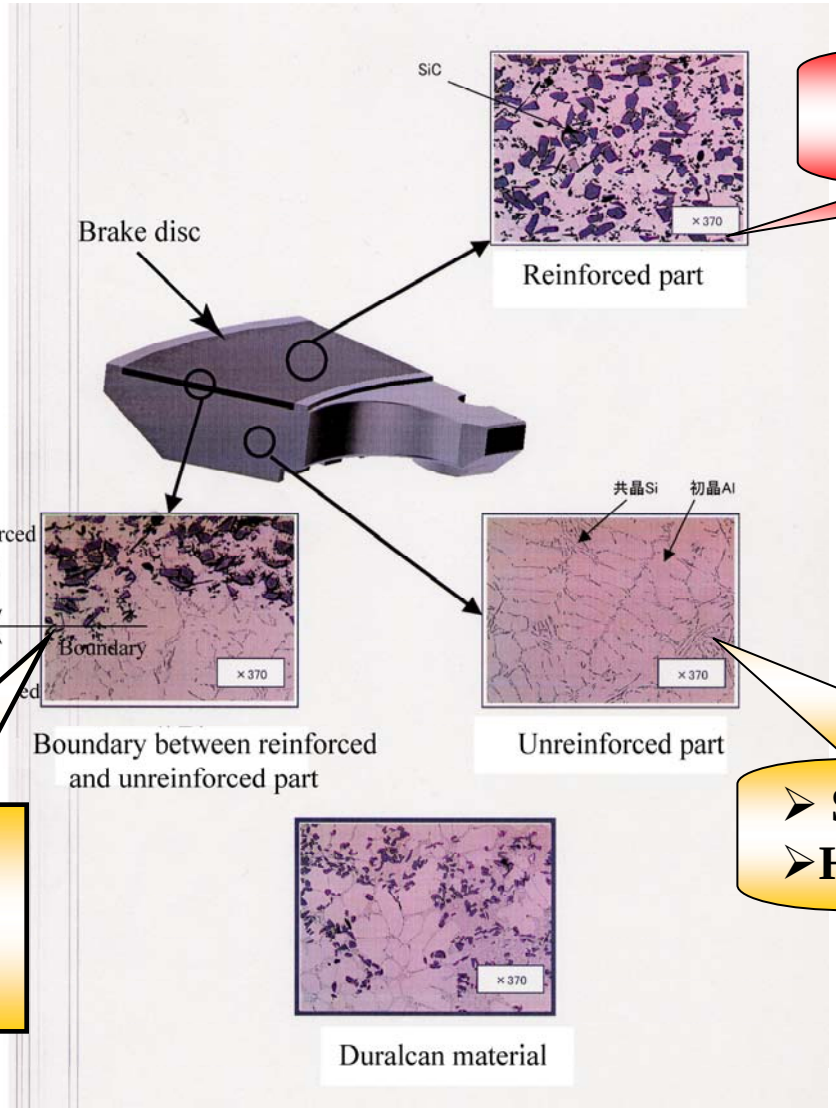

➢ Frictional area
➢Low toughness MMC

➢ Support the whole disc
➢High toughness Al

Strength of this boundary is important!

Fig. Brake disc structure

1.4 Review of the researches

Concept of locally reinforced material for disc brake application

Zeuner et. al. in 1998

- **Manufacturing process**
- **Crack propagation due to cyclic load**

- **Saving of about 52% of material costs**

1.4 Review of the researches

Key mechanism of fracture of MMCs

Christman et al.,1988, 89
Lorca et al., 1991, 92
Levin et al., 1991
Devidson et al., 1993
Chen et al., 2005
Nutt et al.,1987
Arsenault et al., 1985
Tvergaard et al., 1990

- **Ductile fracture**
- **Brittle fracture**
- **Debonding**

Studies of MMC

Cyclic and monotonic fracture mechanism

Studies of locally reinforced hybrid MMC

Fracture mechanism
+
Boundary effect

Not investigated

1.4 Review of the researches

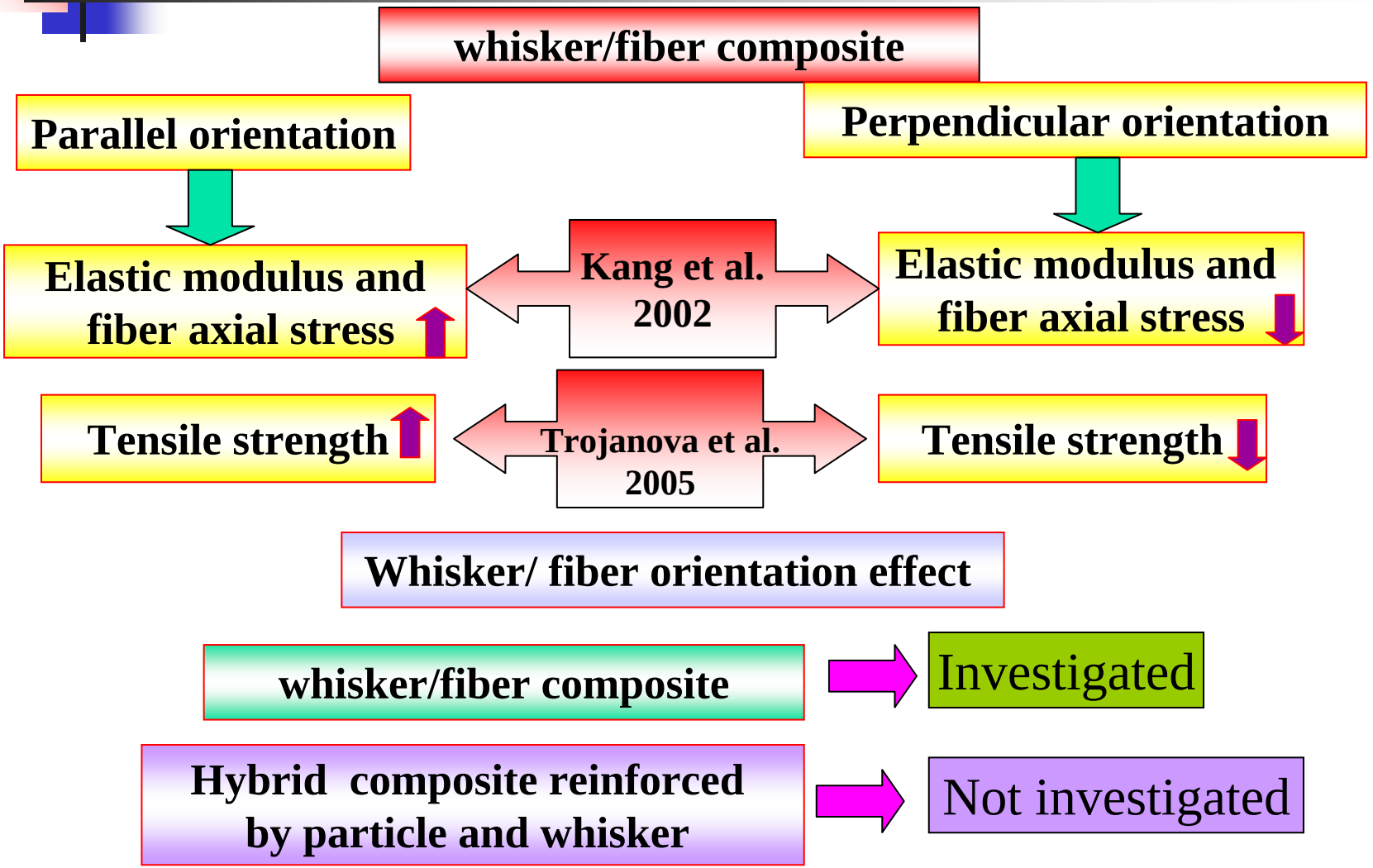

1.5. Motivation of current research

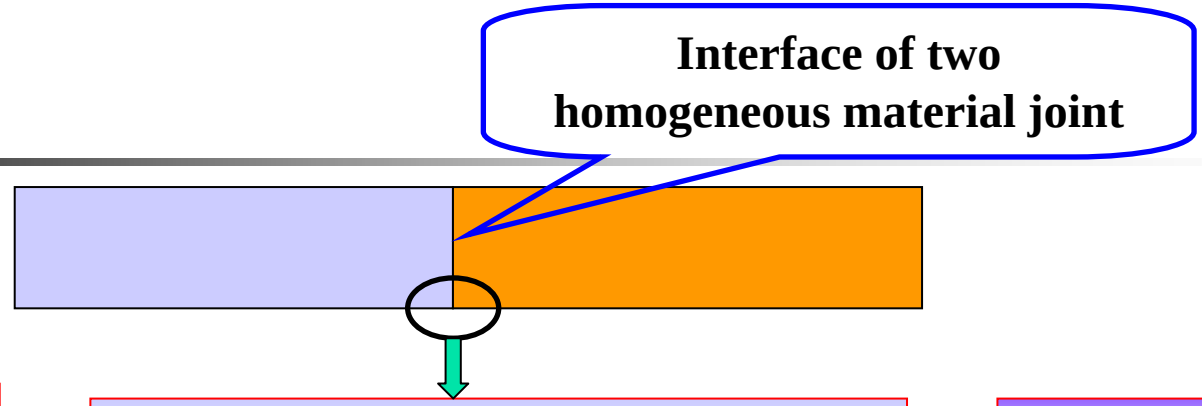

Homogeneous Joint material → Stress concentration at the interface edge → Solved problem

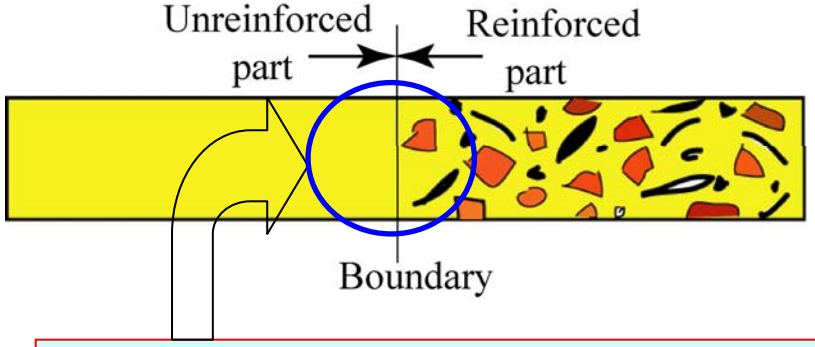

Locally or partially reinforced material → Stress concentration and its influence on fracture behavior → **Unsolved problem**

1.5 Motivation of current research

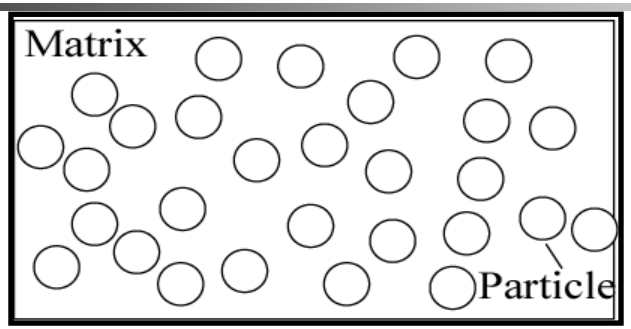

MMC → Monotonic and cyclic fracture behavior → Solved problem

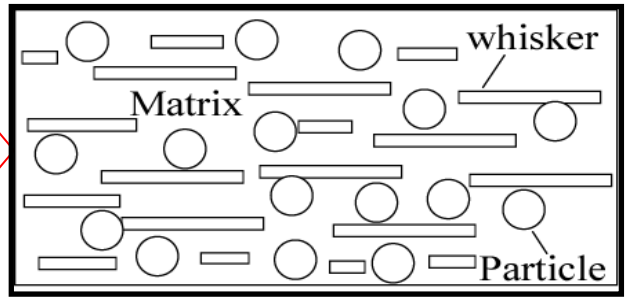

Hybrid MMC → Effect of monotonic and cyclic loading on fracture mechanism → Unsolved problem

1.5 Motivation of current research

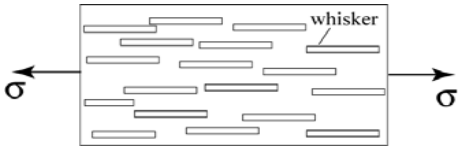

Parallel orientation

Overall strength is high

Fiber/whisker composite

Whisker orientation effect on strength

Solved problem

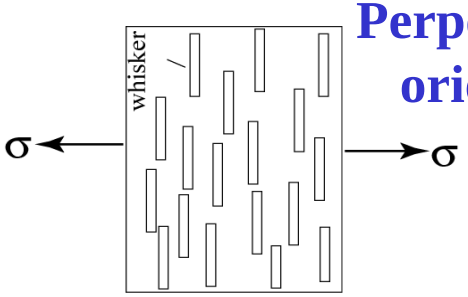

Perpendicular orientation

Overall strength is low

1.5 Motivation of current research

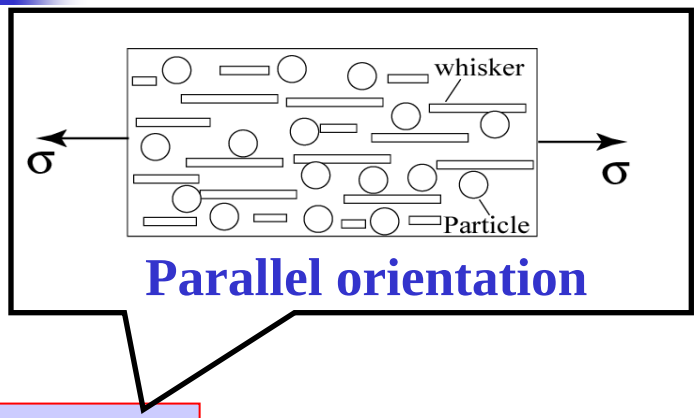

Parallel orientation

Overall strength ?

Hybrid MMC

Whisker orientation effect on strength

Unsolved problem

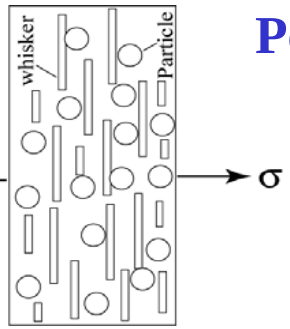

Perpendicular orientation

Overall strength ?

1.6 Scope and objectives

- **To investigate the effect of the boundary between the reinforced part and the unreinforced part on the fracture mechanism under monotonic and cyclic load.**
- **To investigate the effect of monotonic and cyclic load on fracture mechanism.**
- **To investigate the effect of the whisker orientation on the monotonic strength and fatigue strength and its effect on fracture mechanism.**
- **The stress and strain distributions predicted by simulations, using a microscopic mechanical model for the locally reinforced materials, are compared to the experimental observations.**

2. PART-1

Fracture mechanism and stress distribution under monotonic and cyclic load

Presentation outline of part-1

2.1. Materials and Experimental procedure

2.2. Experimental Results and Discussion

2.3. Numerical Analysis

2.1. Materials and Experimental procedure

2.1.1. Material fabrication and specimen preparation

2.1.2. Microstructure observation

2.1.3. Experimental setup and procedure

2.1.4. Summary

2.1.1. Material fabrication and specimen preparation

Material fabrication: Squeeze casting method
Reinforced part:
21 vol.% SiC particles and 9 vol.% Al_2O_3 whiskers as reinforcement
70 vol.% Al alloy as matrix
Unreinforced part: Al alloy

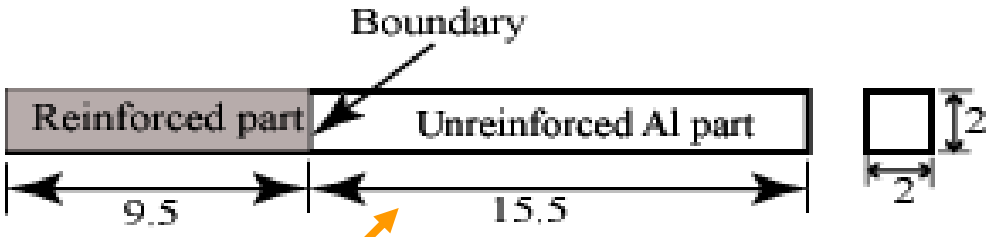

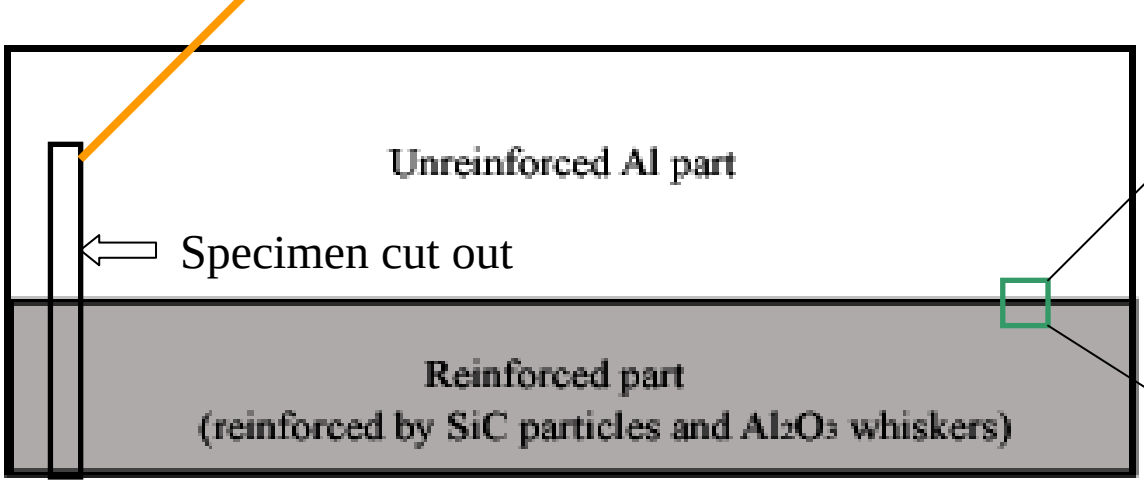

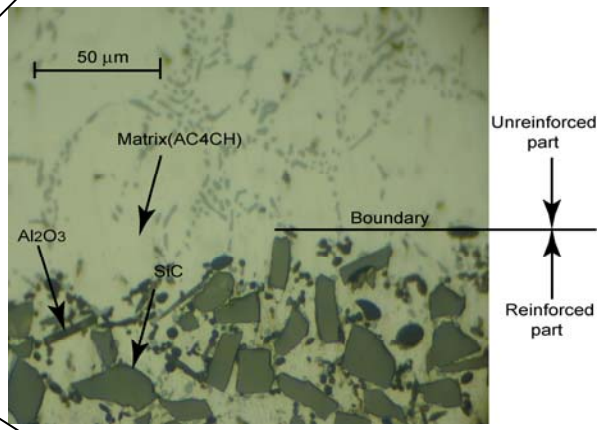

Fig. Specimen cut out from a disc (unit: mm)

2.1.1 Material fabrication and specimen preparation

Table: Volume fraction and mechanical properties

Parameters	Al_2O_3	SiC	AC4CH alloy	MMC
V, %	9	21	70	-
E, GPa	380	450	70.0	142
ν	0.27	0.20	0.33	0.28
σ_{ys}, MPa	-	-	131	166

V: Volume content, E : Young's modulus, ν : Poisson's ratio and σ_{ys} : Yield strength

Table: Chemical composition of Al alloy (wt.%)

Si	Fe	Mg	Ti	Al
7.99	0.2 MAX	0.57	0.07	Bal.

2.1.2 Microstructure observation

SiC particle: Rectangular shape and average grain diameter 23 μm
Al_2O_3 whisker: Roller shape and average length 33 μm, average diameter 2 μm

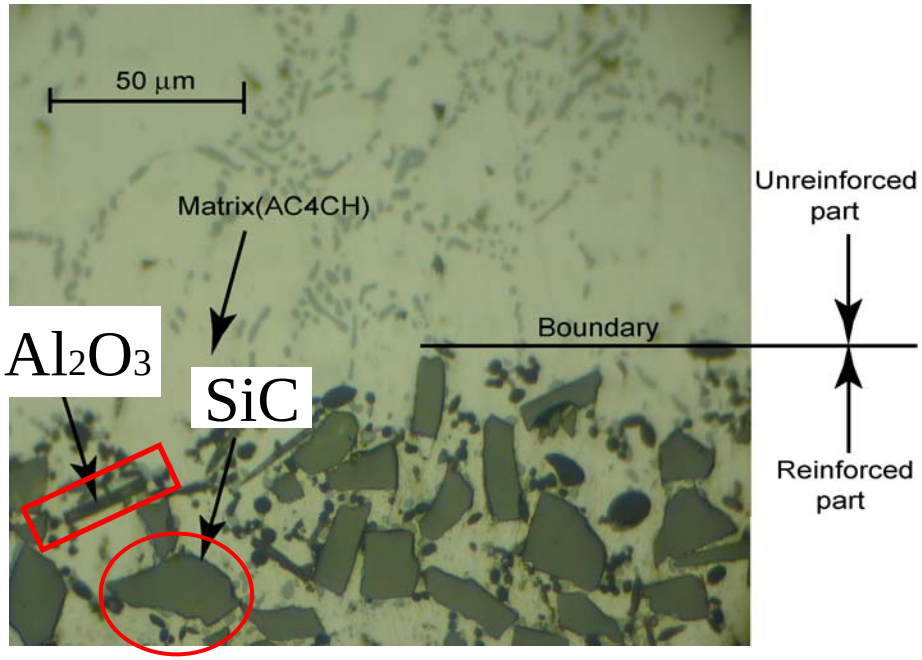

(a) High magnification

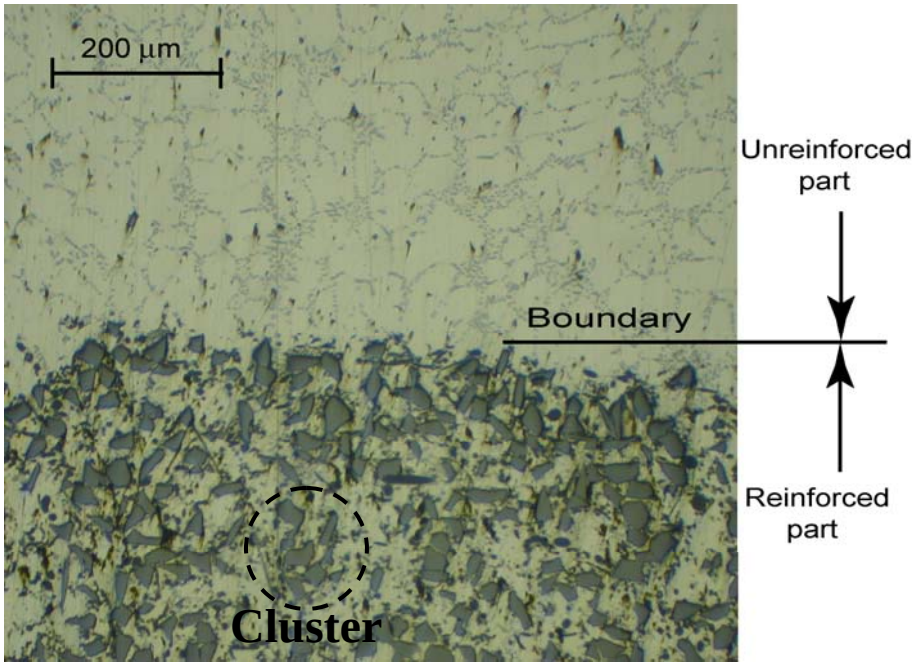

(b) Low magnification

Fig. Optical microscope photographs of the specimen around the boundary between the reinforced part and the unreinforced part.

2.1.3. Experimental setup and Procedure

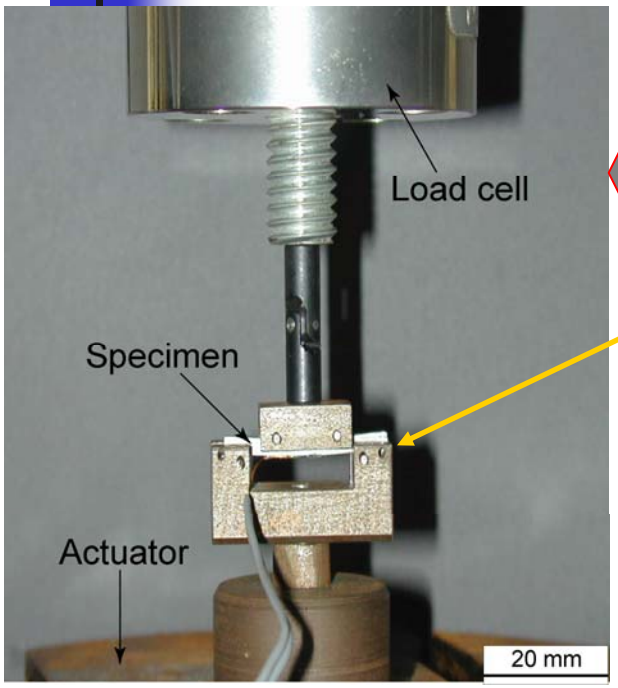

Fig. An experimental setup

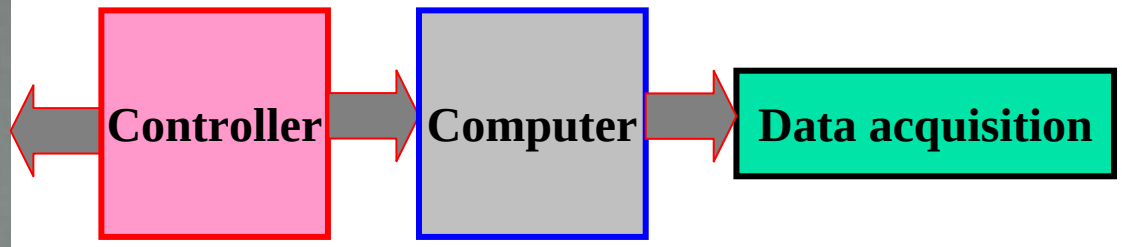

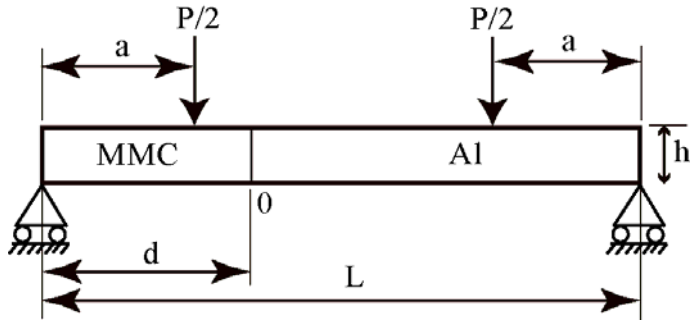

Four-point bending

Load cell: 980N
Inner span: 10 mm
Outer span: 20 mm

2.1.3 Experimental setup and Procedure

Test conditions

1. **Monotonic test:**
   - **Displacement rate of 0.0025 mm/s.**

2. **Cyclic test:**
   - **Stress ratio: R = 0.1 (R= $\sigma_{min}/\sigma_{max}$)**
   - **Frequency: 1 to 10 Hz**
   - **Wave form of the load: sine wave**

Fracture surface observation

- **Scanning Electron Microscope (SEM)**
- **Energy Dispersive X-ray analysis (EDX)**

2.1.4 Summary

- Material fabrication: Hybrid preforms with squeeze casting method
- There is no sharp interface between the reinforced and the unreinforced part
- SEM and EDX analysis is used to determine microstructure fracture mode

2.2 Experimental results and discussion

2.2.1 Monotonic test results

2.2.2. Fatigue test results

2.2.3 Summary

2.2.1 Monotonic test results

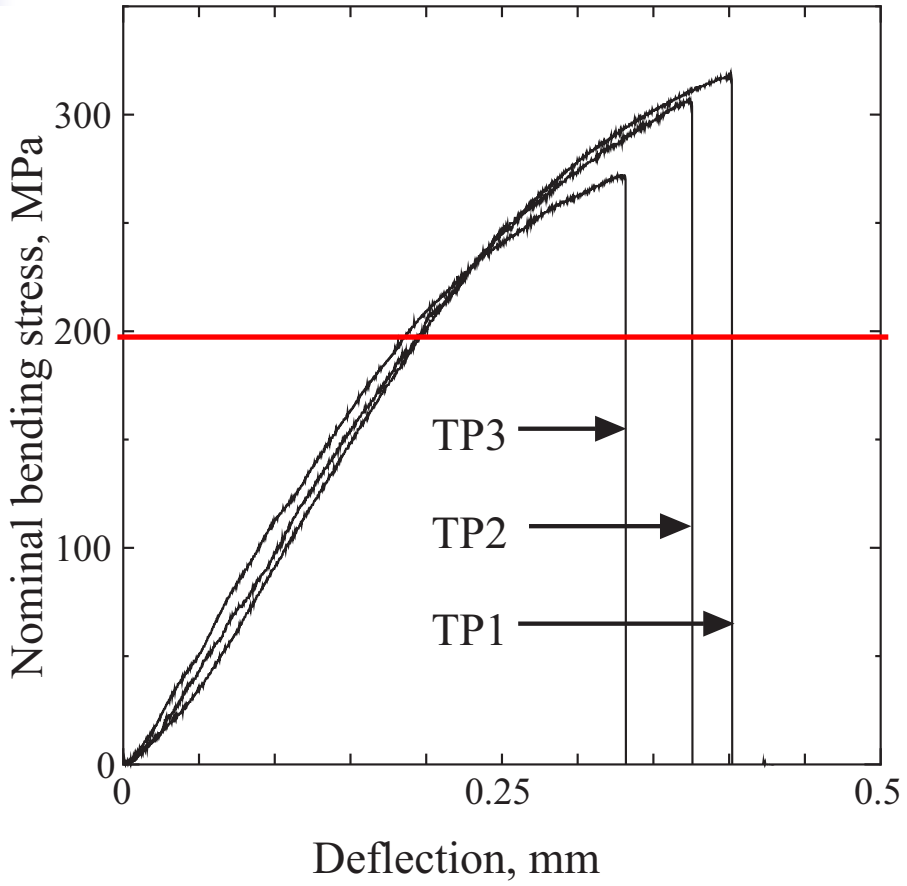

Average bending strength
298 MPa

Fig. Nominal bending stress versus deflection curves under monotonic loading.

2.2.1 Monotonic test results

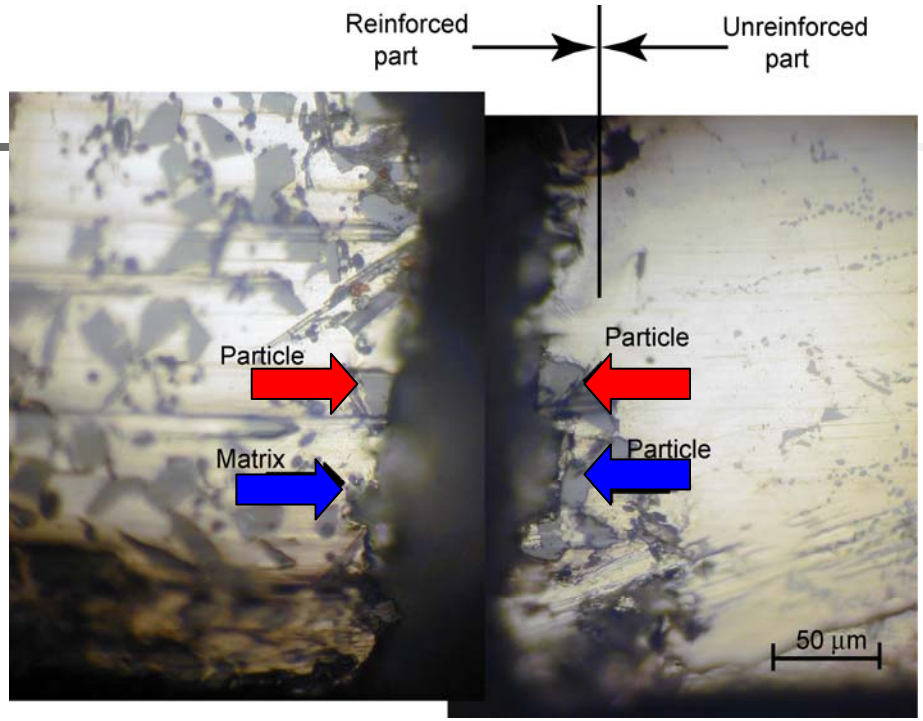

Fig. Matching surface view of fractured specimen under monotonic loading, TP3

Table: Fracture stresses and minimum distance from the fracture location to macroscopic boundary between reinforced part and unreinforced part under monotonic loading

Specimen	σ_f, MPa	Boundary-fracture distance
TP1	318	2 particles (46 μm)
TP2	306	1 particle (23 μm)
TP3	272	1 particle (23 μm)

2.2.1 Monotonic test results

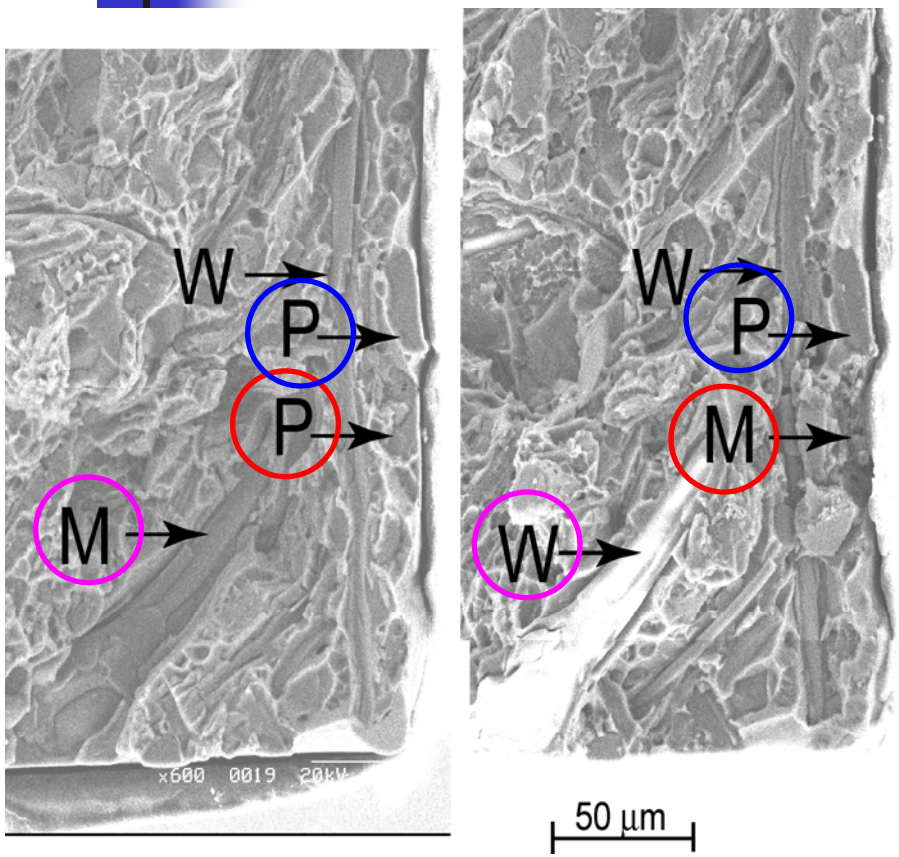

Fig. Matching fracture surface of locally reinforced material under monotonic loading, TP3

Table: Area fraction of SiC particle and Al_2O_3 whisker fracture and interface debonding between SiC particle-matrix and Al_2O_3 whisker-matrix under monotonic and cyclic loading condition

Load type	SiC particle		Al_2O_3 whisker	
	F, %	D, %	F, %	D, %
Monotonic	10.5	10.1	0.85	9.3
Cyclic	1.9	19.0	0.85	8.9

F is fracture area and D is debonding area

2.2.2 Fatigue test results

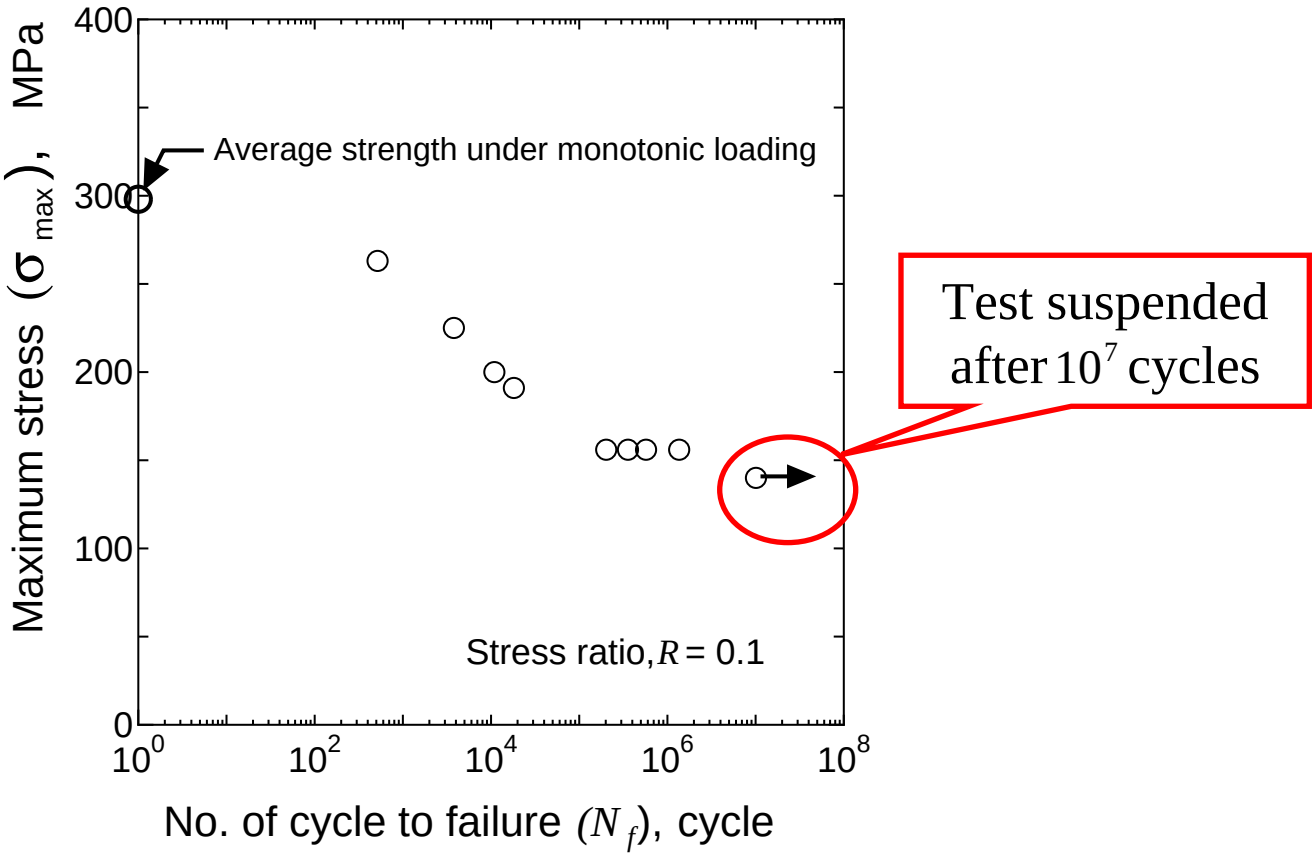

Fig. Stress versus fatigue life behavior (stress ratio, =0.1).

2.2.2 Fatigue test results

Table : Fatigue life and distance from fatigue fracture location to macroscopic boundary

Specimen	σ_{max}, MPa	N_f, cycle	Boundary-fracture distance
CTP1	261	517	2 particles (46 μm)
CTP2	225	3781	0.11mm
CTP3	200	1.08×10^4	0.13 mm
CTP4	191	1.8×10^4	0.34 mm
CTP5	156	5.73×10^5	0.23 mm
CTP6	156	3.56×10^5	0.26 mm
CTP7	156	2.02×10^5	0.31 mm
CTP8	156	1.30×10^6	0.35 mm

2.2.2 Fatigue test results

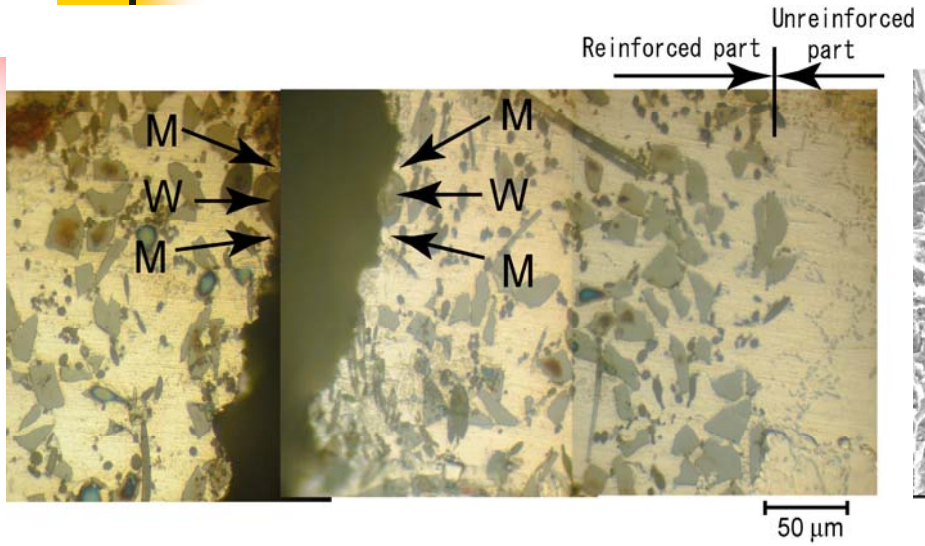

Fig. Matching surface view of fatigue fractured specimen under cyclic loading, maximum stress 156 MPa.

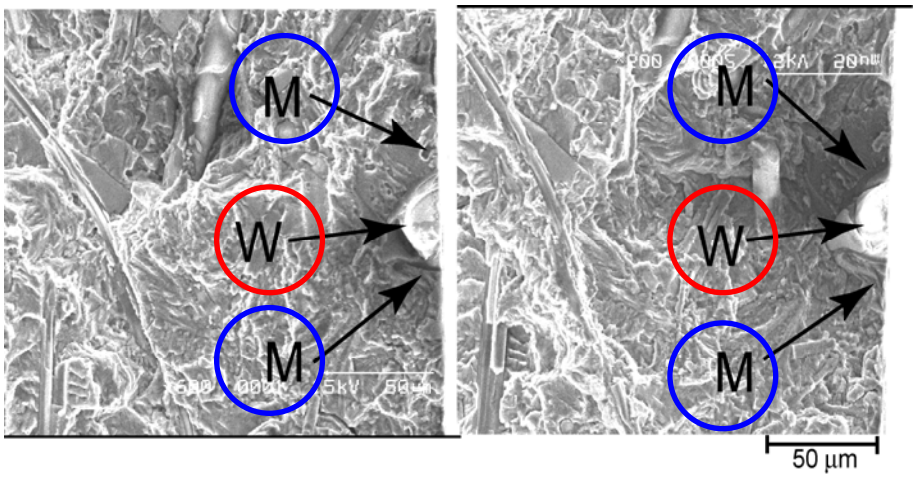

Fig. Matching fracture surface after fatigue fracture, maximum stress 156MPa**.**

Table: Area fraction of SiC particle and Al_2O_3 whisker fracture and interface debonding between SiC particle-matrix and Al_2O_3 whisker-matrix under monotonic and cvclic loading condition

Load type	SiC particle		Al_2O_3 whisker	
	F, %	D, %	F, %	D, %
Monotonic	10.5	10.1	0.85	9.3
Cyclic	1.9	19.0	0.85	8.9

F is fracture area and D is debonding area

2.2.3 Summery of experimental results

Monotonic:

- Average monotonic strength 298 MPa
- Specimen broken at first or second closest particle to unreinforced part
- Fracture occurred in the particle as well as the particle/matrix or whisker/matrix interface under monotonic loading

Fatigue:

- Fatigue fracture occurs under the maximum stress above one half of the monotonic fracture stress.
- In the low maximum stress, fracture location is far from the boundary. however, when the maximum stress is high fracture location is very close to the macroscopic boundary
- Fracture surface is dominated by particle/matrix and whisker/matrix interfacial debonding.

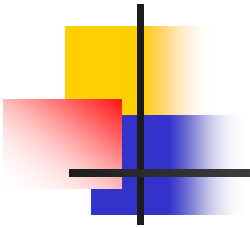

2.3 Numerical Analysis

2.3.1 Numerical model

2.3.2. Numerical results and discussion

2.3.3 Summary of numerical analysis

2.3.1 Numerical model

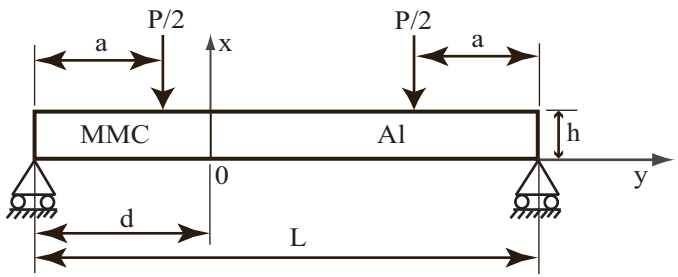

Fig. Global model of homogeneous materials joint.

Displacement field

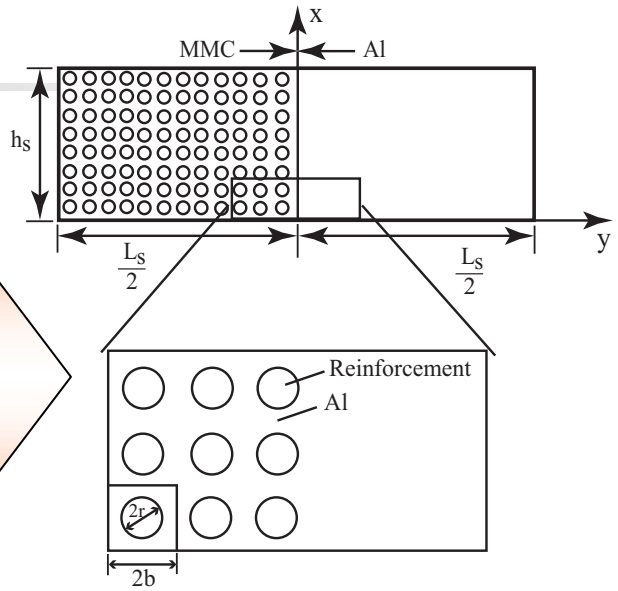

Table: Geometry of numerical mode (Unit: mm)

Model	L, L_s	h, h_s	a	d	2r	2b
Global model	20.0	2.0	5.0	7.0	-	-
Sub model	1.48	0.444	-	-	0.023	0.037

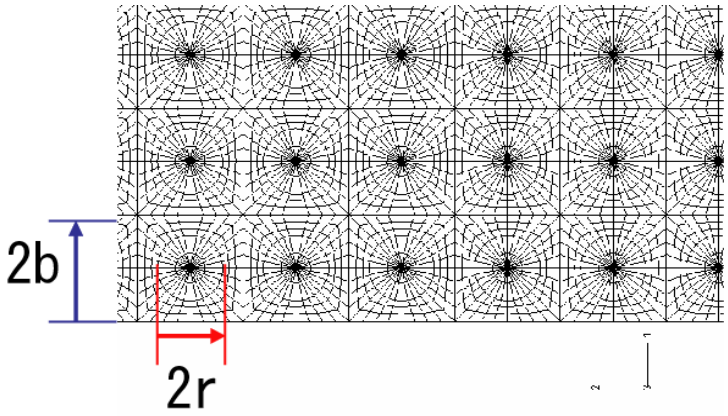

Fig. Inclusion array model with mesh division

2.3.2 Numerical results and discussion

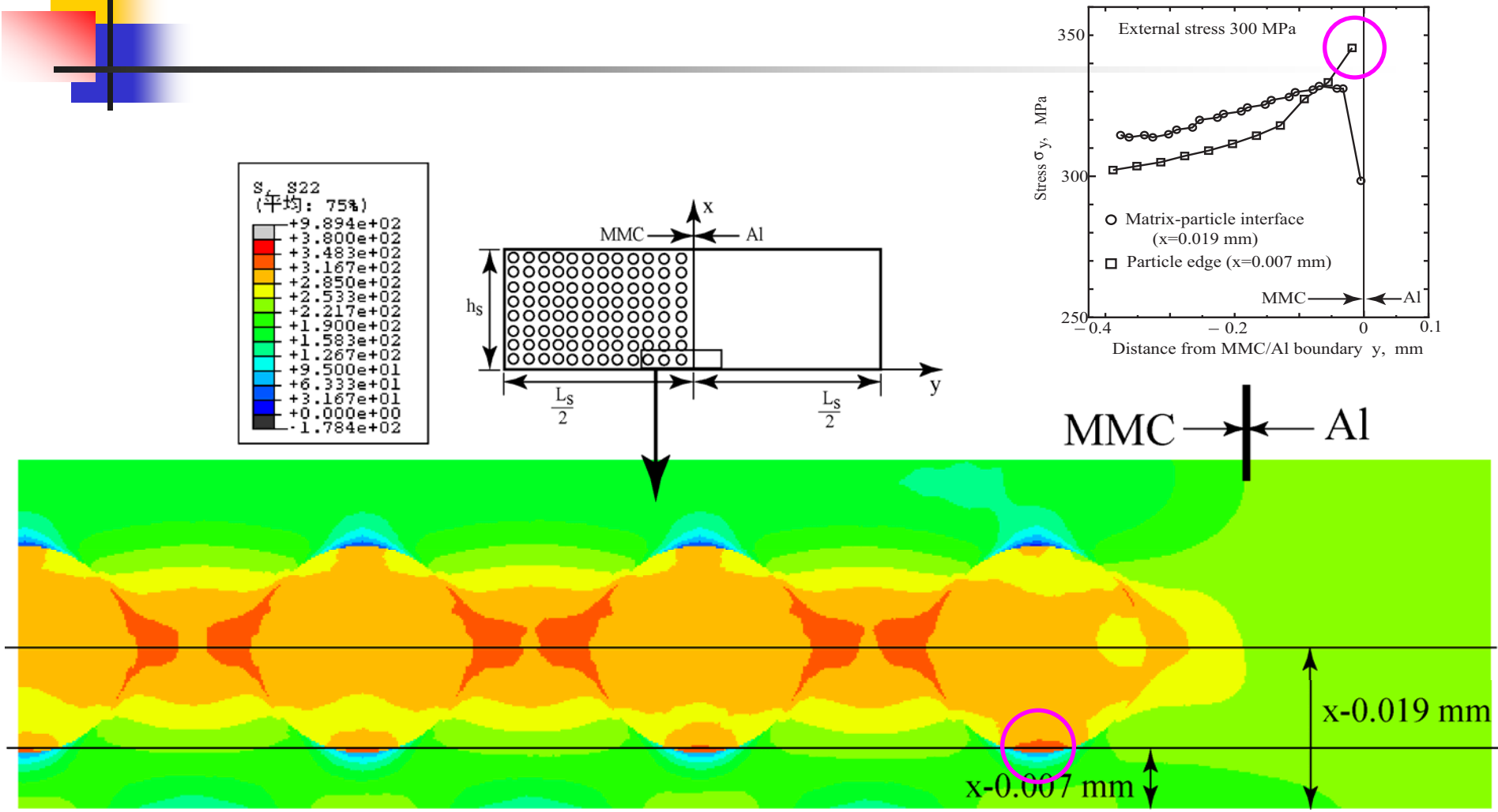

Fig. Stress distributions along y direction of inclusion array model under nominal bending stress 300 MPa.

2.3.2 Numerical results and discussion

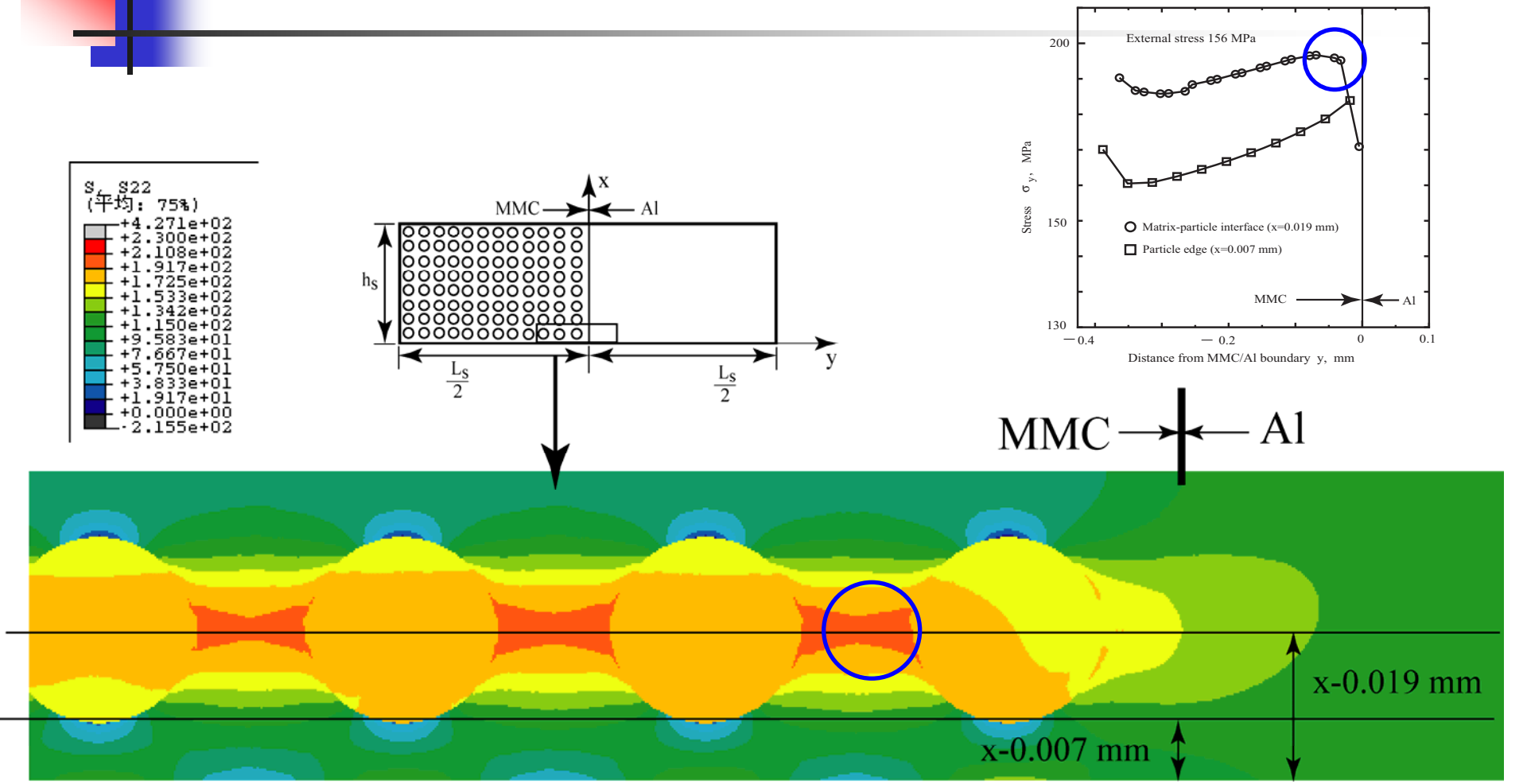

Fig. Stress distributions along y direction of inclusion array model under nominal bending stress 156 MPa.

2.3.2 Numerical results and discussion

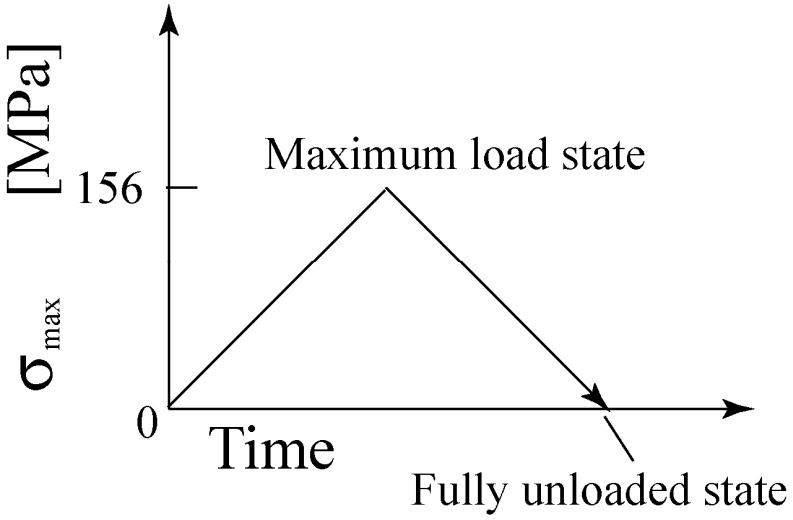

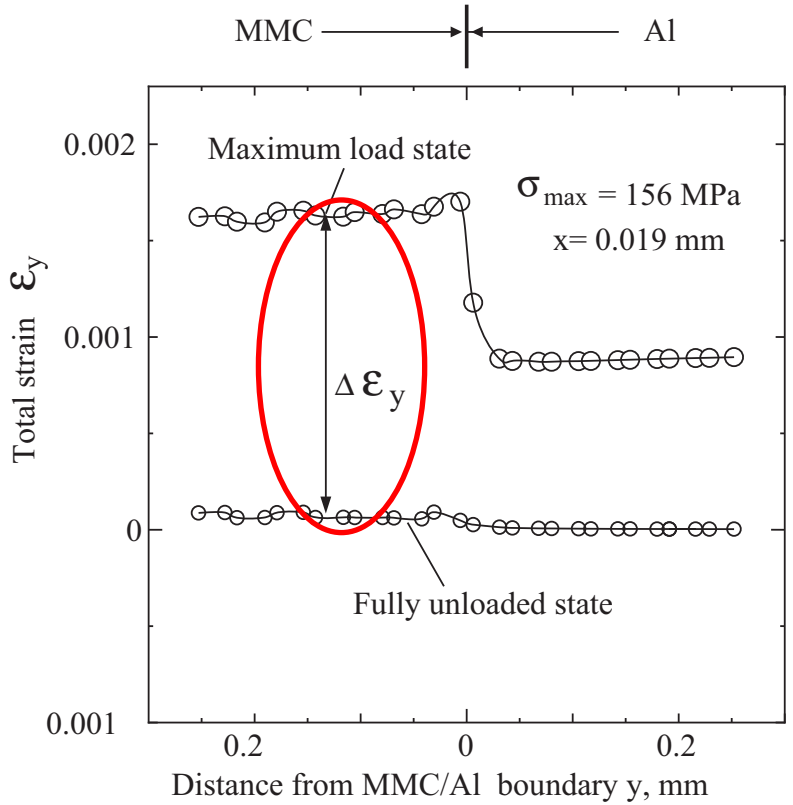

Fig. Distributions of total strain in matrix along normal to the boundary of inclusion array model under cyclic loading at maximum stress 156 MPa.

2.3.3 Summary of numerical analysis

- Peak stress develops at the first inclusion edge in the high nominal stress case (corresponding to the monotonic load) .
- Peak stress develops at the interface between the inclusion and matrix alloy in the low nominal stress case (corresponding to the cyclic load).
- The predicted strain amplitude is much higher in the reinforced side compare to the unreinforced side.

3. PART-2

Effect of whisker orientation on monotonic and fatigue strength

Presentation outline of part-2

3.1. Specimen preparation

3.2. Experimental results and discussion

3.3. Numerical analysis

3.1. Material fabrication and specimen preparation

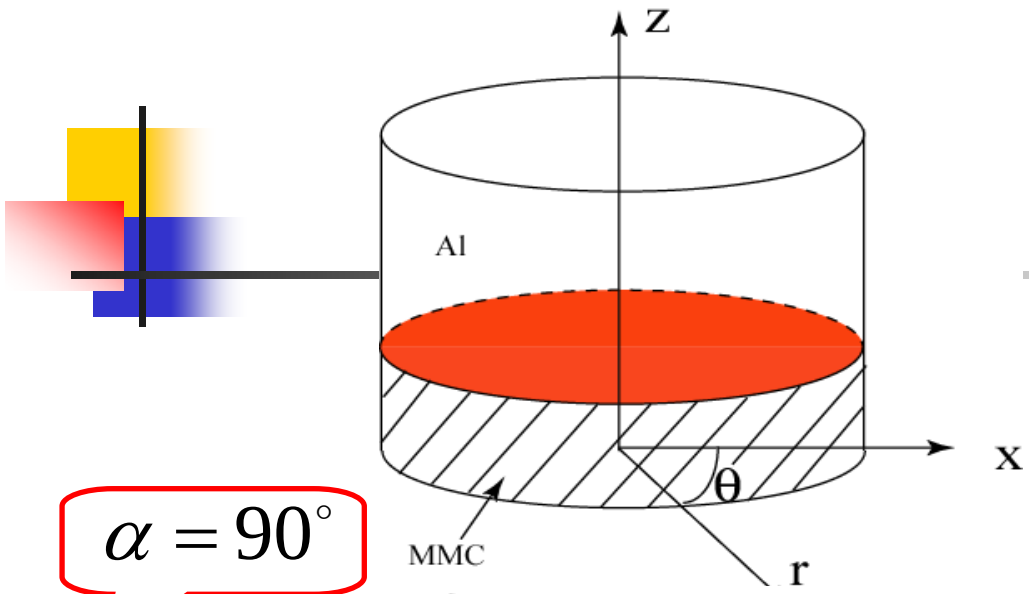

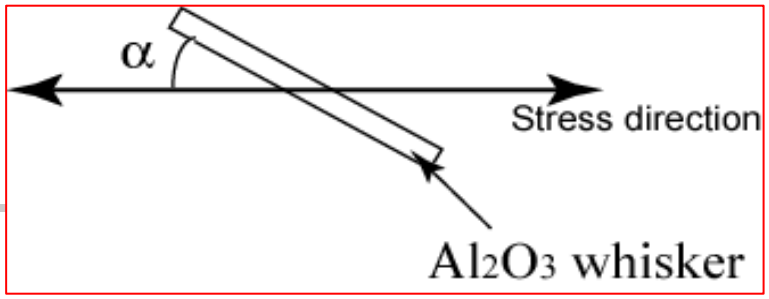

$\alpha = 90^\circ$

$\alpha = 0^\circ \sim 90^\circ$

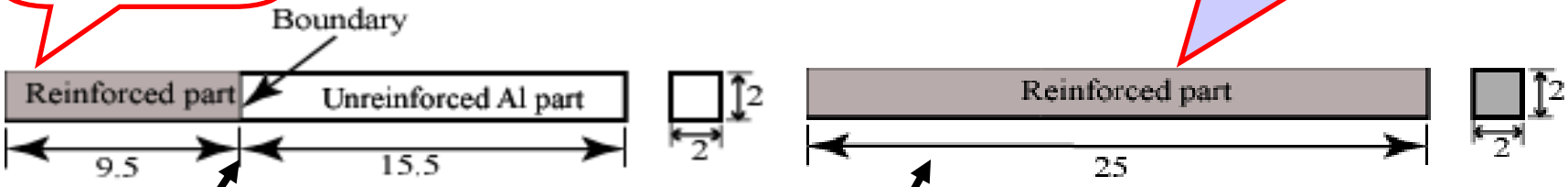

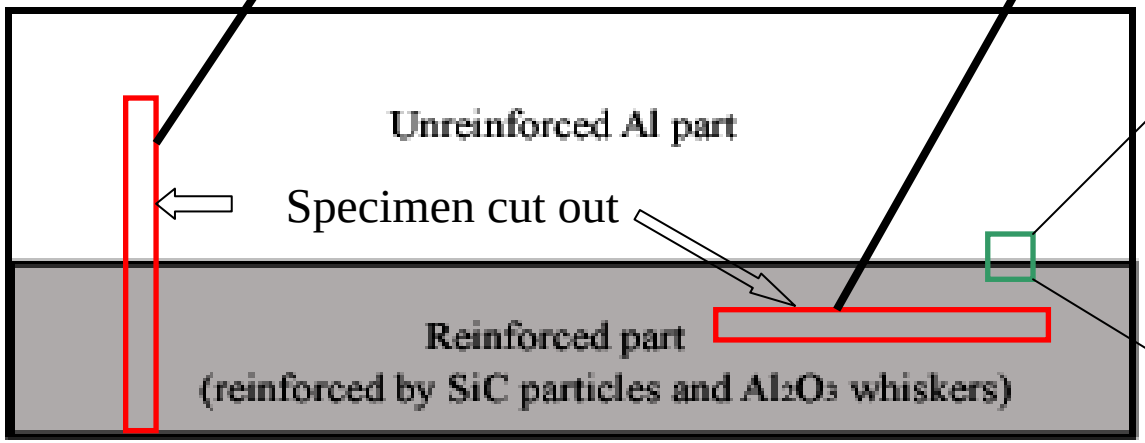

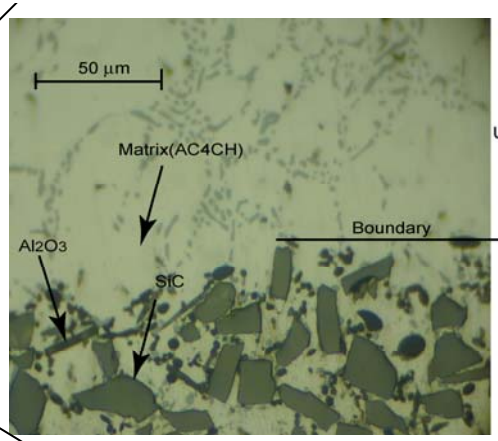

Disc

3.1. Specimen preparation

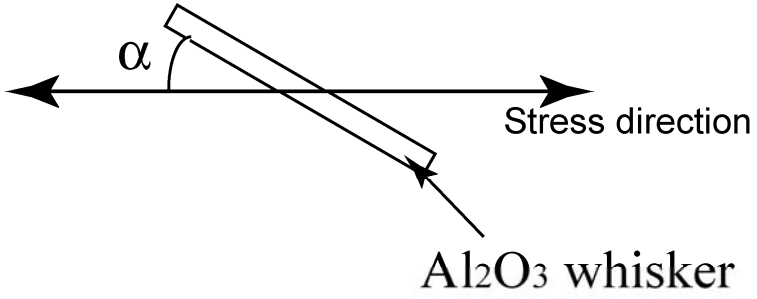

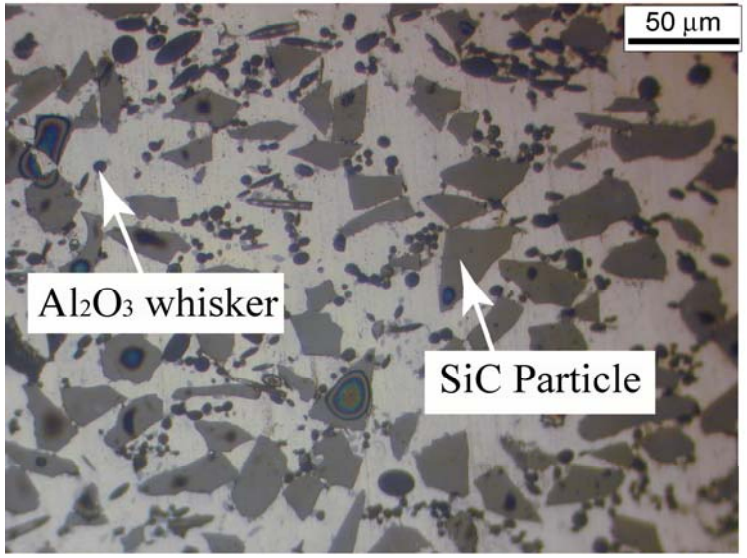

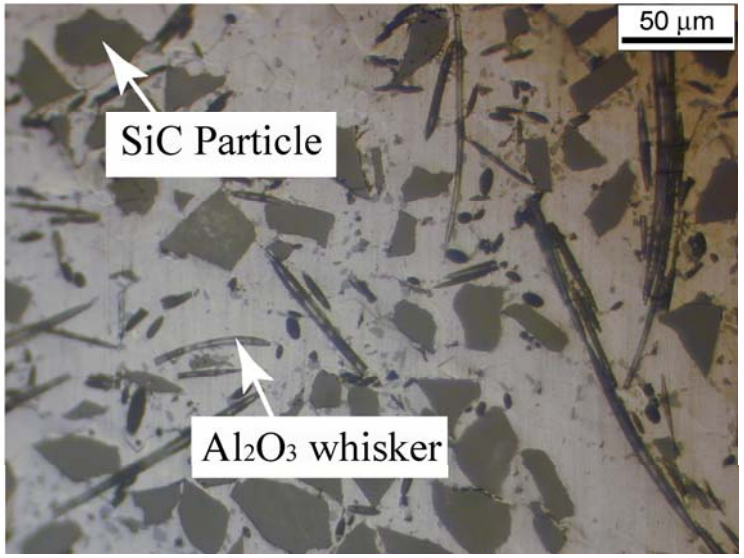

$\alpha = 90^\circ$

$\alpha = 0^\circ \sim 90^\circ$

Fig. Optical micrograph of the composite on the tensile side face

3.2. Experimental results and discussion

3.2.1. Monotonic test results

3.2.2. Fatigue test results

3.2.3. Fracture surface observation

3.2.4. Summary

3.2.1. Monotonic test results

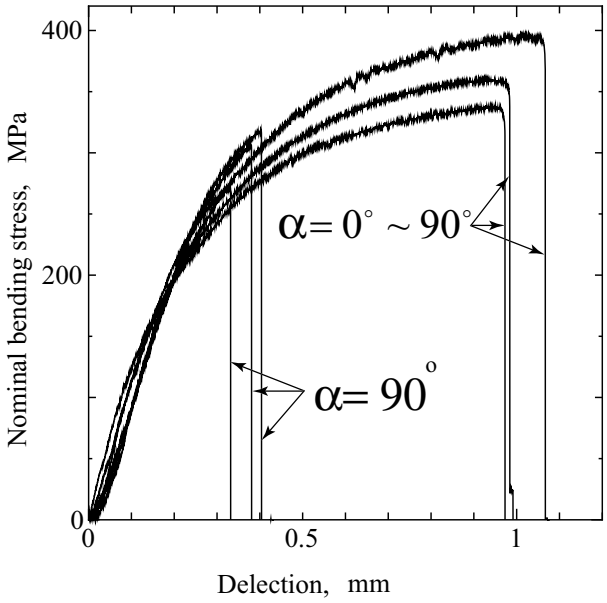

Fig. Nominal bending stress versus deflection curves under monotonic loading.

$\alpha = 90^{\circ}$
Average bending strength
298 MPa

$\alpha = 0^{\circ} \sim 90^{\circ}$
Average bending strength
364 MPa

21%SiCp+9% Al_2O_3
18% higher

5%SiCp+15% Al_2O_3
(Z. Trojanova et.all, 2005)
16% higher strength for parallel orientation $\alpha = 0^{\circ}$

3.2.2. Fatigue test results

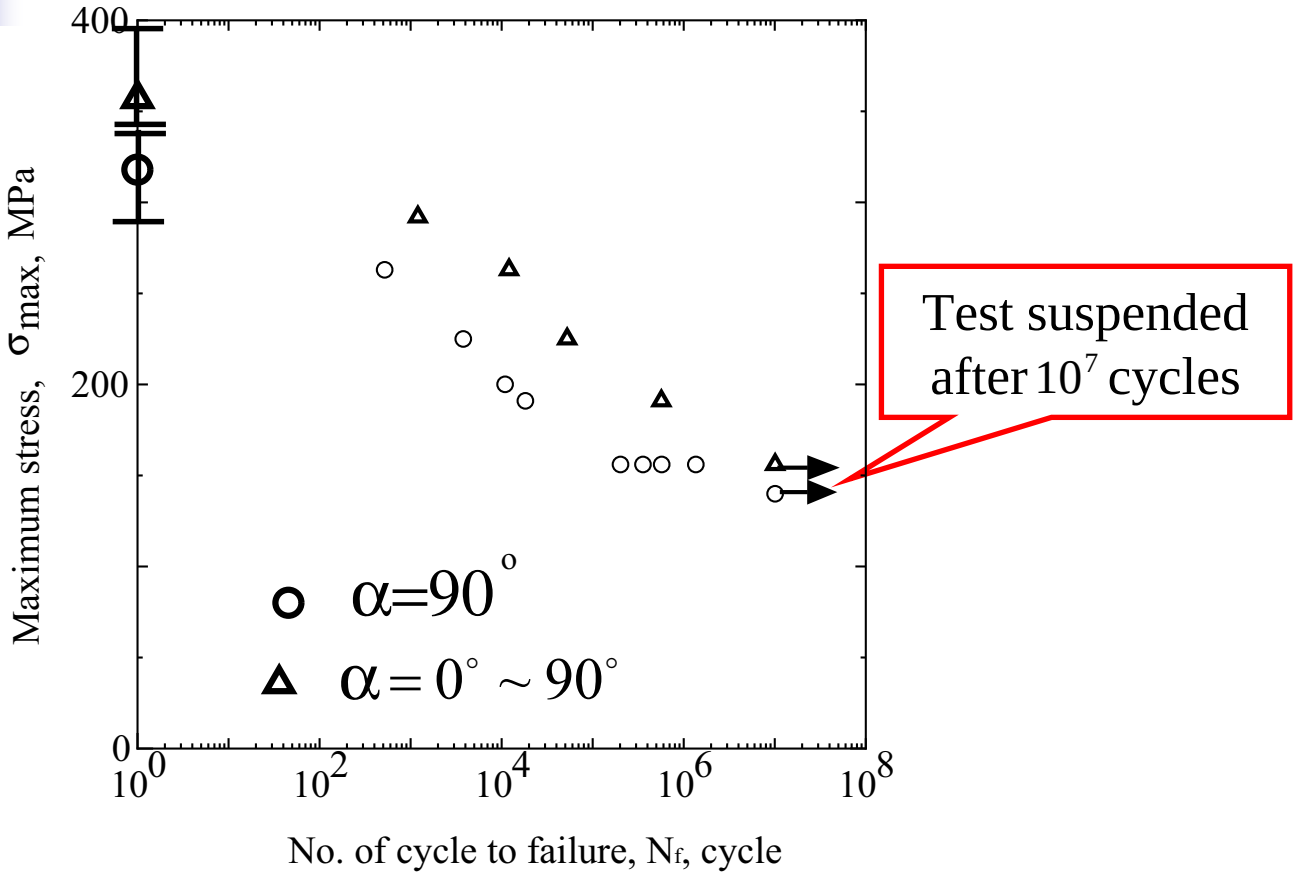

Fig. Stress versus fatigue life behavior (stress ratio, R=0.1). The plots on N_f =0 show average strength under monotonic load.

3.2.3. Fracture surface observation

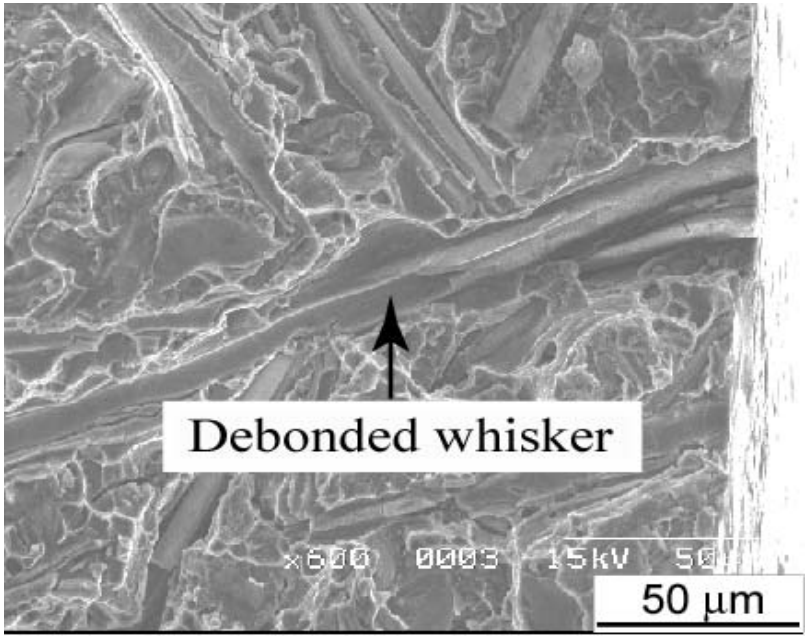

$(\alpha = 90^\circ)$

Table: Area fraction of SiC particle and Al_2O_3 whisker farcture/debonding under cyclic loading condition

Material	SiC particle		Al_2O_3 whisker	
	F, %	D, %	F, %	D, %
α=90°	1.2	19.6	0.6	9.1
α=0° – 90°	1.9	20.6	11	0.1

F is fracture area and D is debonding area

Fig. Fracture surface under cyclic loading condition

3.2.3. Fracture surface observation

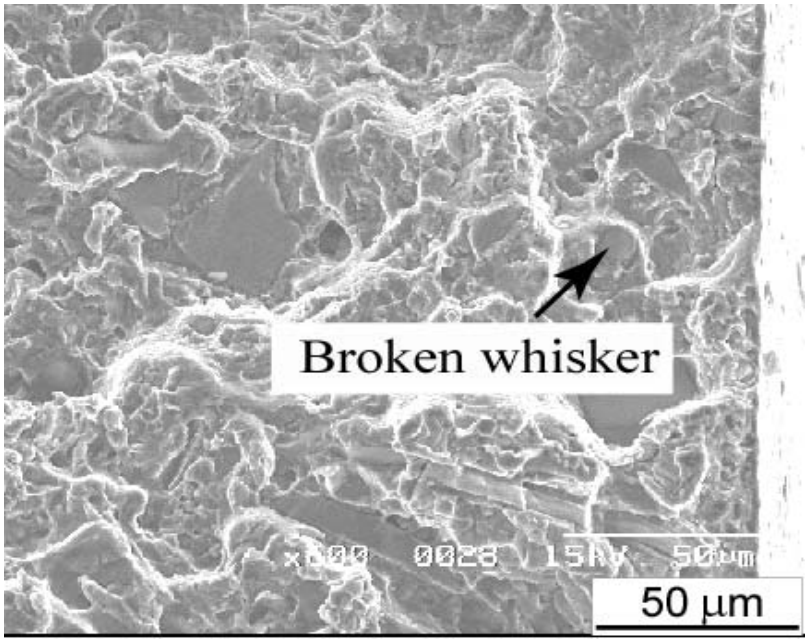

$\alpha = 0^\circ \sim 90^\circ$

Table: Area fraction of SiC particle and Al_2O_3 whisker farcture/debonding under cyclic loading condition

Material	SiC particle		Al_2O_3 whisker	
	F, %	D, %	F, %	D, %
α=90°	1.2	19.6	0.6	9.1
α=0° – 90°	1.9	20.6	11	0.1

F is fracture area and D is debonding area

Fig. Fracture surface under cyclic loading condition

3.2.3. Fracture surface observation

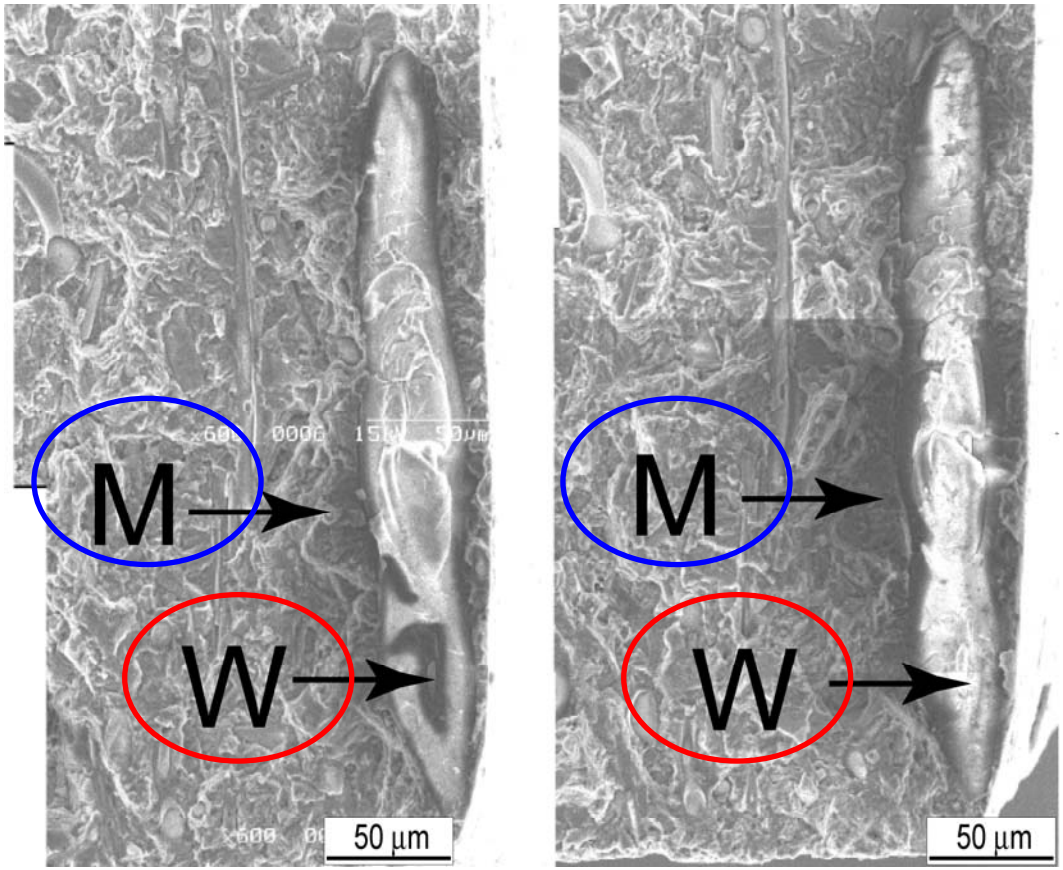

Fig. Matching fatigue fracture surface $\alpha = 0^\circ \sim 90^\circ$

$\sigma_{\max} = 191$ MPa, $N_f = 67617.$

3.2.3 Fracture surface observation

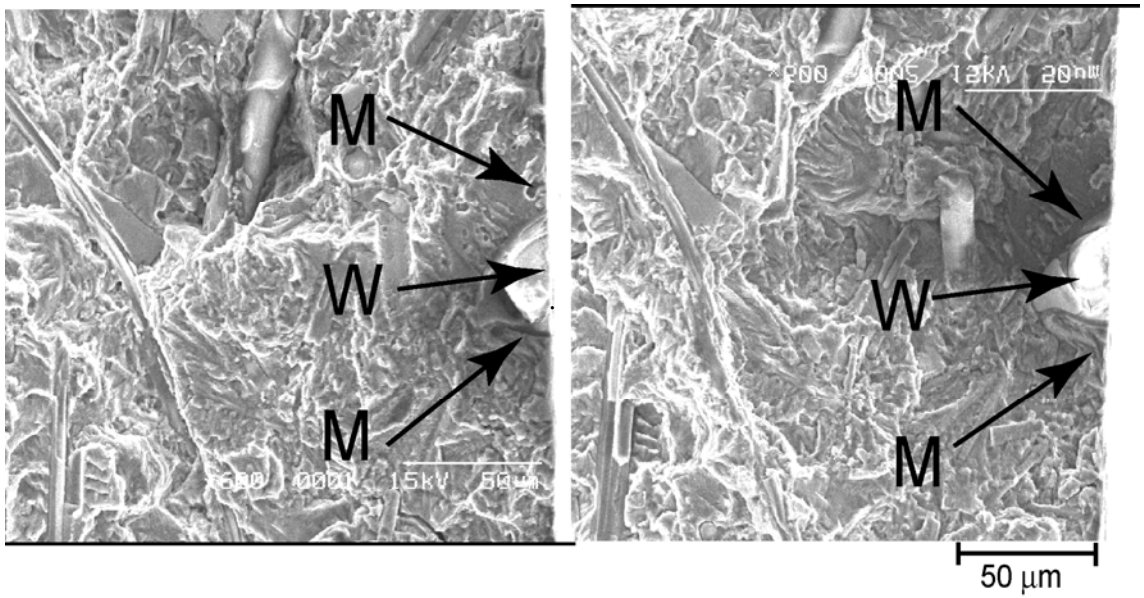

Fig. Matching fracture surface $(\alpha = 90^{\circ})$

$$\sigma_{\max} = 156 \text{ MPa}, \quad N_f = 5.73 \times 10^5$$

3.2.4. Summary of experimental results

- **When $\alpha = 0^\circ \sim 90^\circ$, both monotonic and fatigue strength is higher than $(\alpha = 90^\circ)$**

- **When the whisker direction is perpendicular $(\alpha = 90^\circ)$ to the stress direction almost all whiskers are debonded.**

- **When the whisker direction is random $\alpha = 0^\circ \sim 90^\circ$ to the stress direction almost all whiskers are broken.**

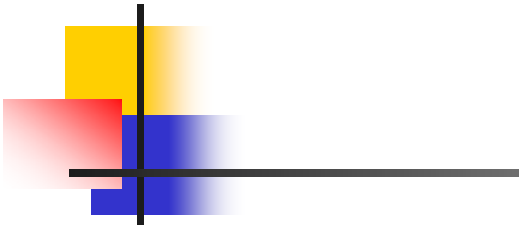

3.3. Numerical analysis

3.3.1. Numerical model

3.3.2. Numerical results and discussion

3.3.3. Summary

3.3.1 Numerical model

Whisker composite model

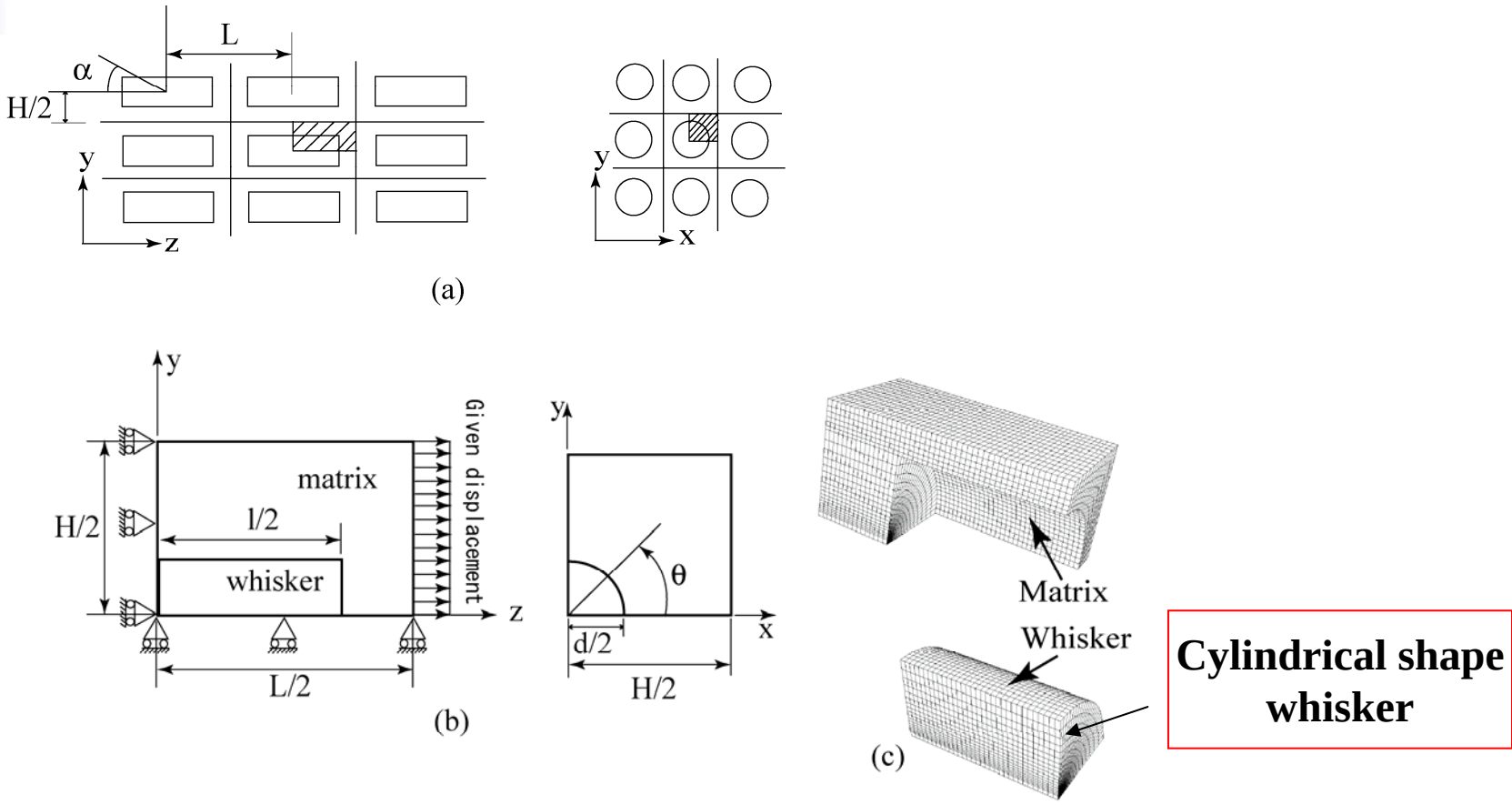

Fig. 3-D single whisker model representing the whisker reinforced Al alloy (a) and (b) schematic illustration of the fiber arrangement (c) finite-element mesh.

3.3.1 Numerical model

Periodic Boundary Condition

$u_z = 0, \quad \tau_{zy} = \tau_{zx} = 0 \quad$ on z = 0

$u_x = 0, \quad \tau_{xz} = \tau_{xy} = 0 \quad$ on x= 0

$u_y = 0, \quad \tau_{yz} = \tau_{xy} = 0 \quad$ on y= 0

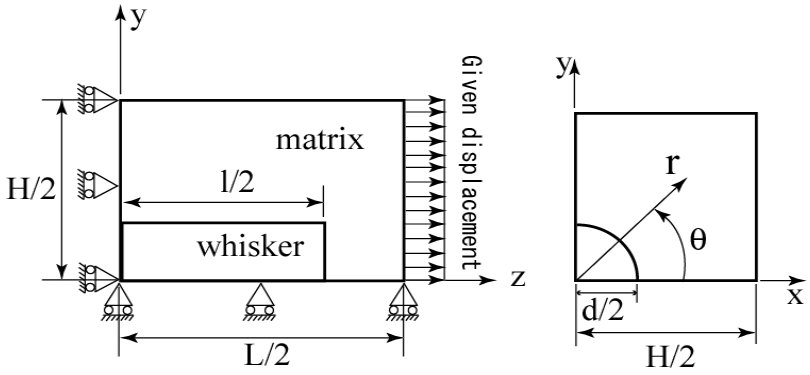

$$u_z = \varepsilon_{ave} L/2, \quad \int_{x=0}^{x=H/2}\int_{y=0}^{x=H/2} \tau_{xz} dxdy = 0, \quad \iint \tau_{zy} dxdy = 0 \quad \text{on z= L/2} \qquad (4)$$

$$u_y = U_y, \quad \tau_{yz} = \tau_{xy} = 0, \quad \int_{z=0}^{z=L/2}\int_{x=0}^{x=H/2} \tau_{yx} dxdz = 0, \iint \tau_{yz} dxdz = 0 \quad \text{on} \quad \text{y= H/2} \qquad (5)$$

$$u_x = U_x, \quad \tau_{xz} = \tau_{xy} = 0, \quad \int_{z=0}^{z=L/2}\int_{y=0}^{y=H/2} \tau_{xz} dydz = 0, \iint \tau_{xy} dydz = 0 \quad \text{on} \quad \text{x= H/2} \qquad (6)$$

Where ε_{ave} is the macroscopic strain, U_y and U_x are constant which are determined such that the shear component of traction is free.

3.3.1 Numerical model

Hybrid composite model

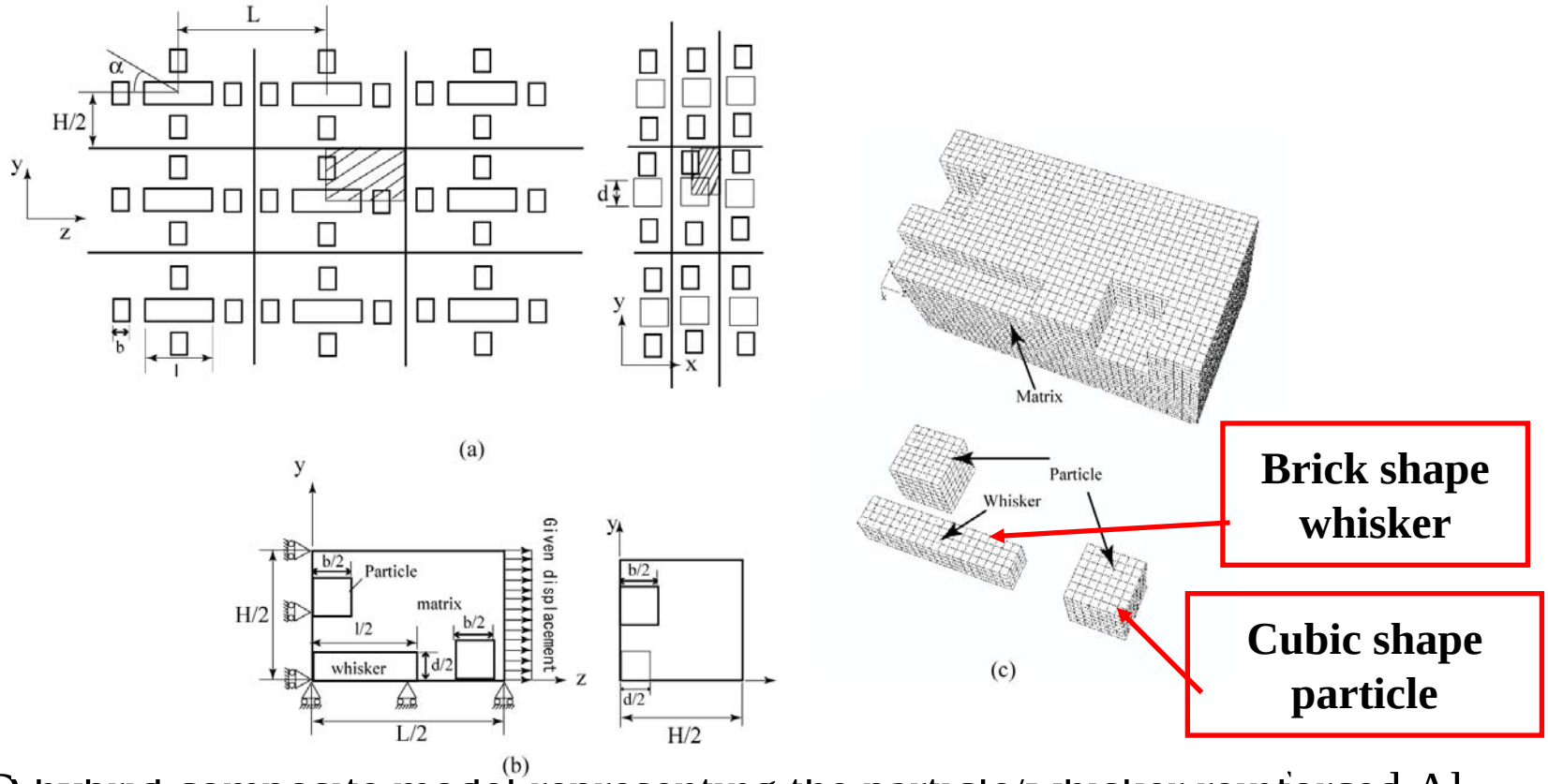

Fig. 3-D hybrid composite model representing the particle/whisker reinforced Al alloy (a) and (b) schematic illustration of the fiber arrangement (c) finite-element mesh.

3.3.2 Numerical results and discussion

Hybrid composite model

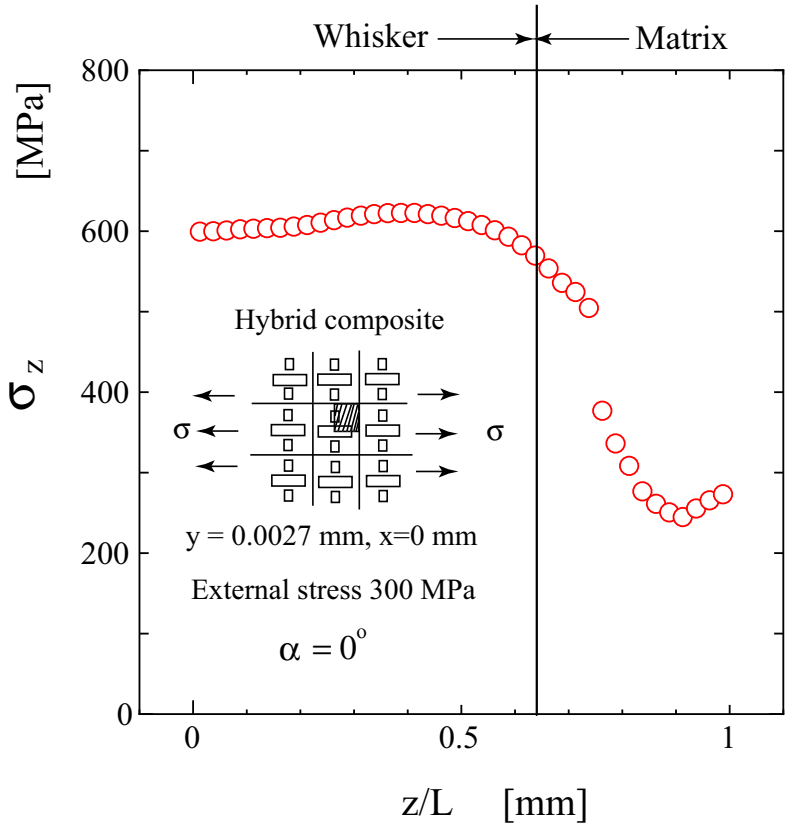

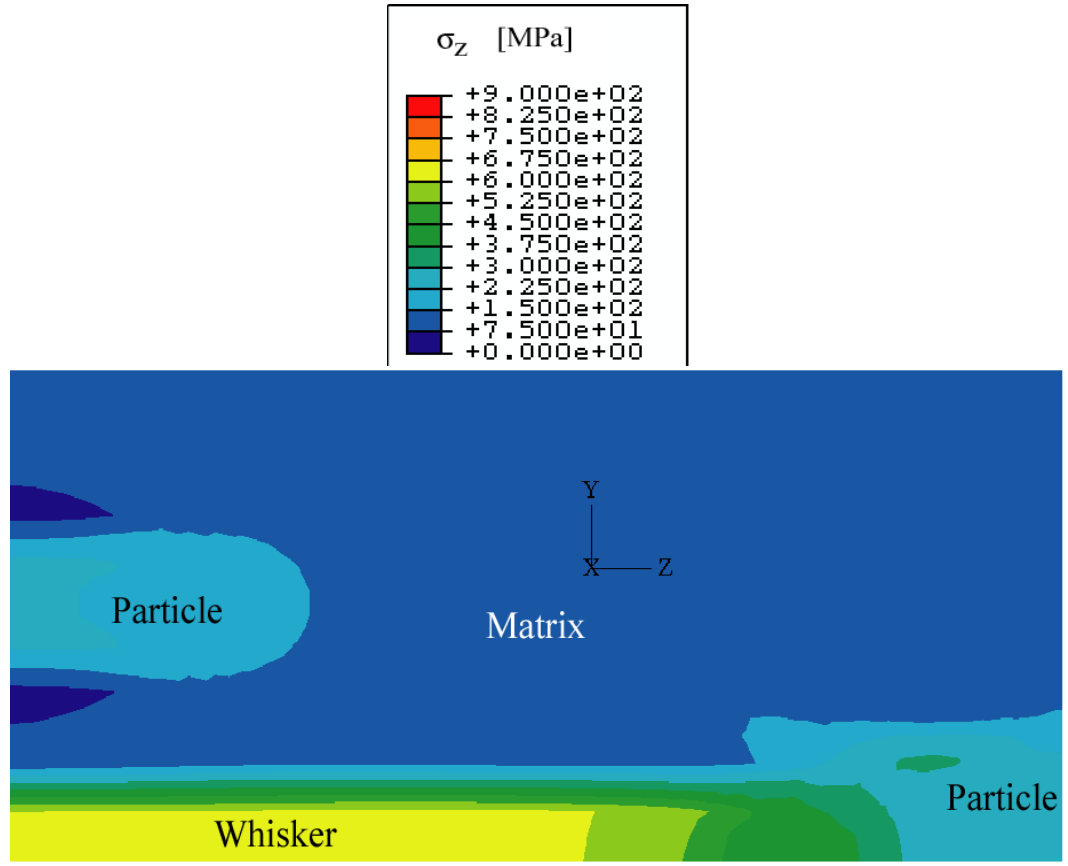

Fig. Stress distribution along Z direction for longitudinal loading (parallel to the stress direction)

3.3.2 Numerical results and discussion

Hybrid composite model

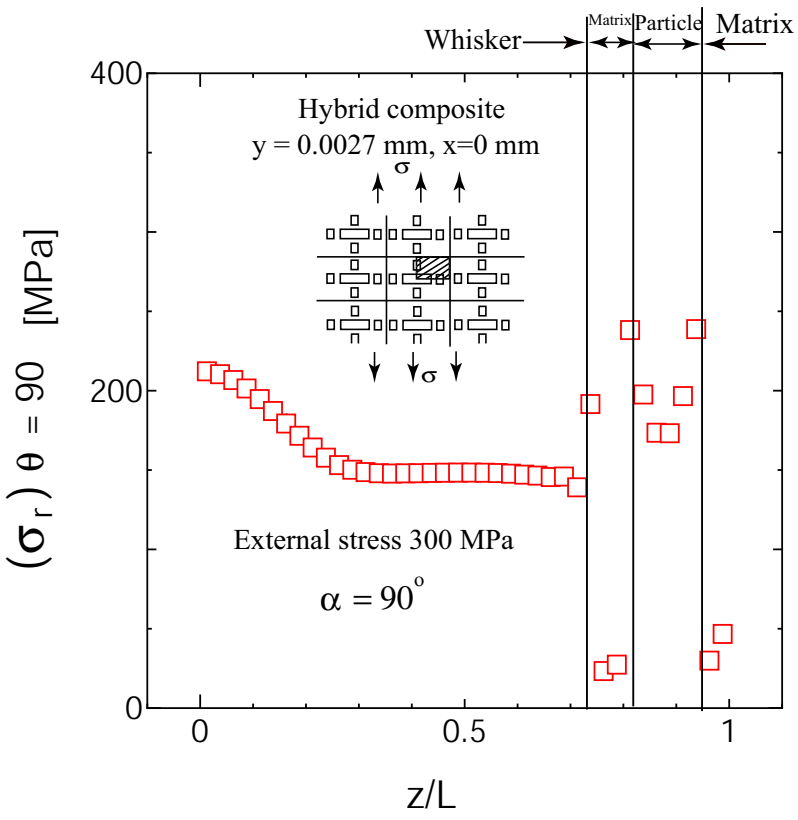

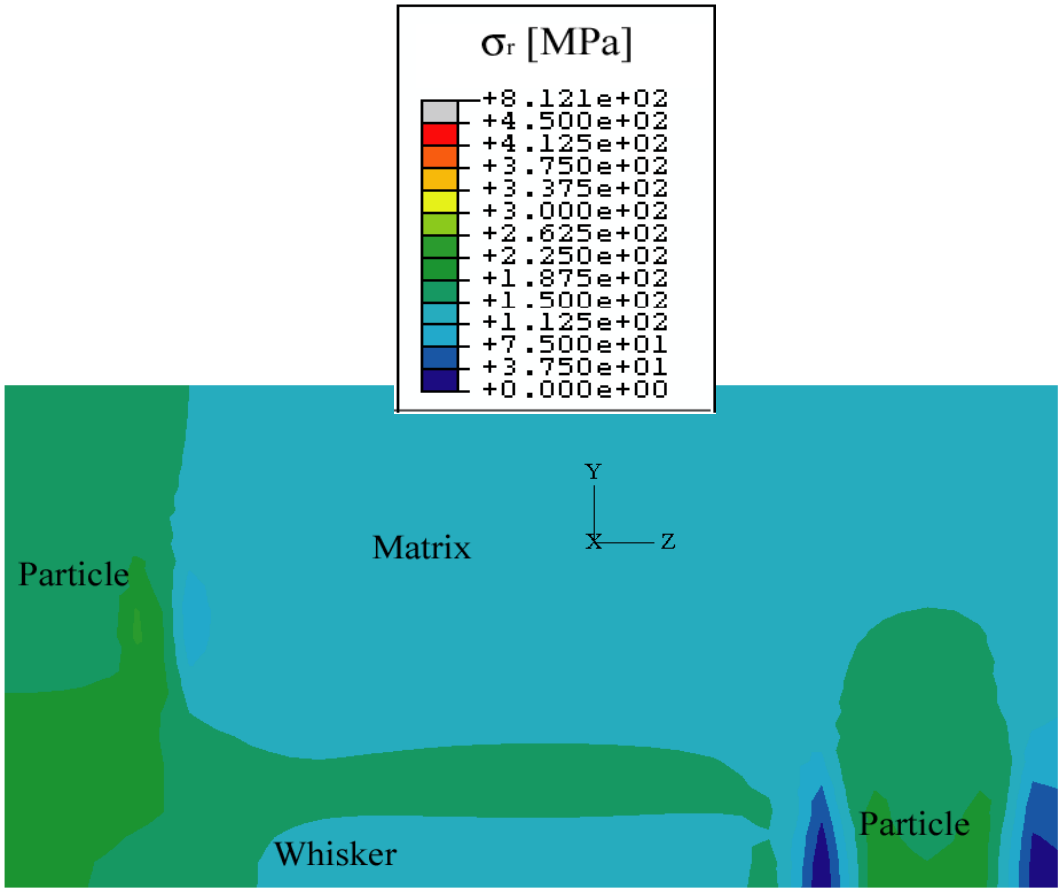

Fig. Stress distribution along θ direction for longitudinal loading (parallel to the stress direction)

3.3.2 Numerical results and discussion

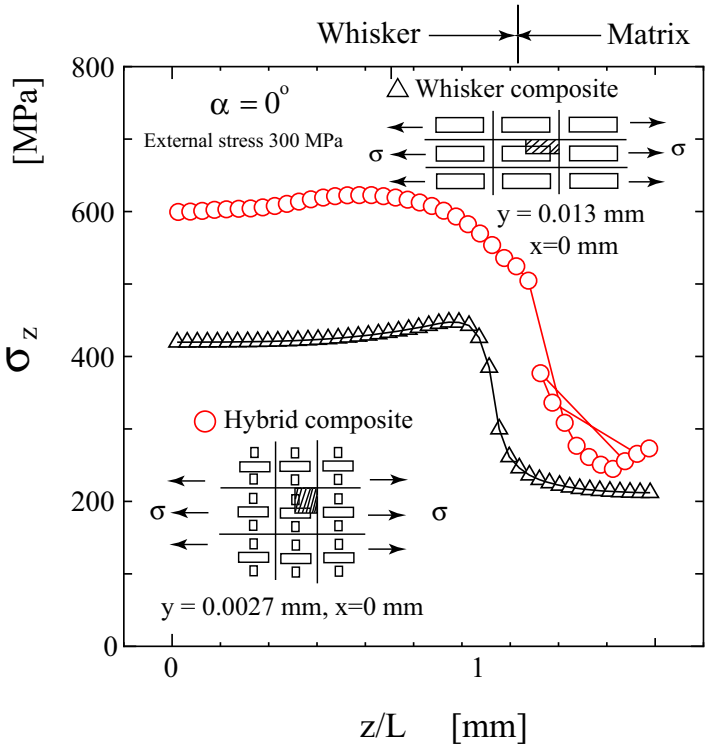

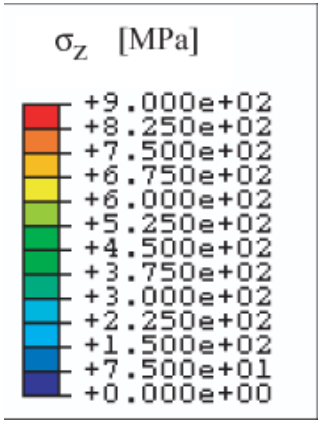

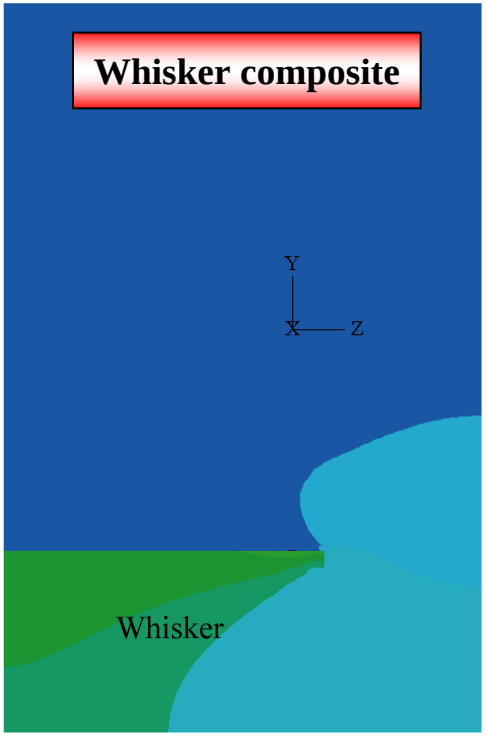

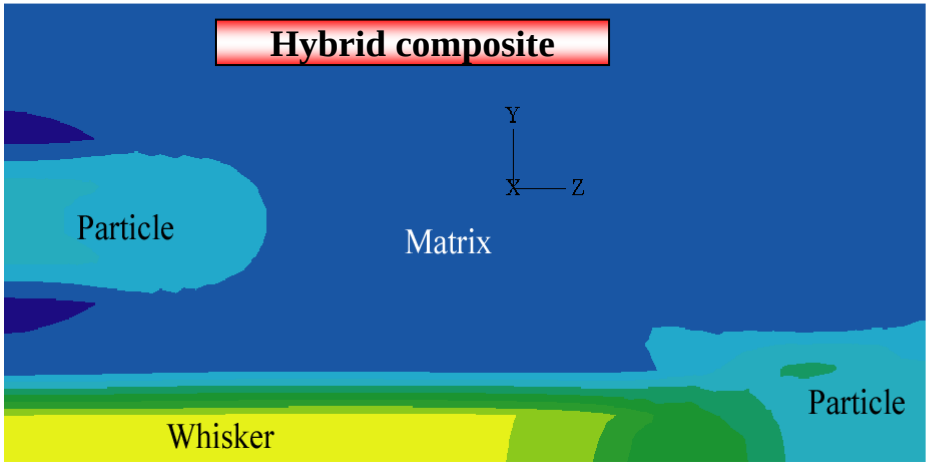

Fig. Stress distribution along Z direction for longitudinal loading (parallel to the stress direction)

3.3.2 Numerical results and discussion

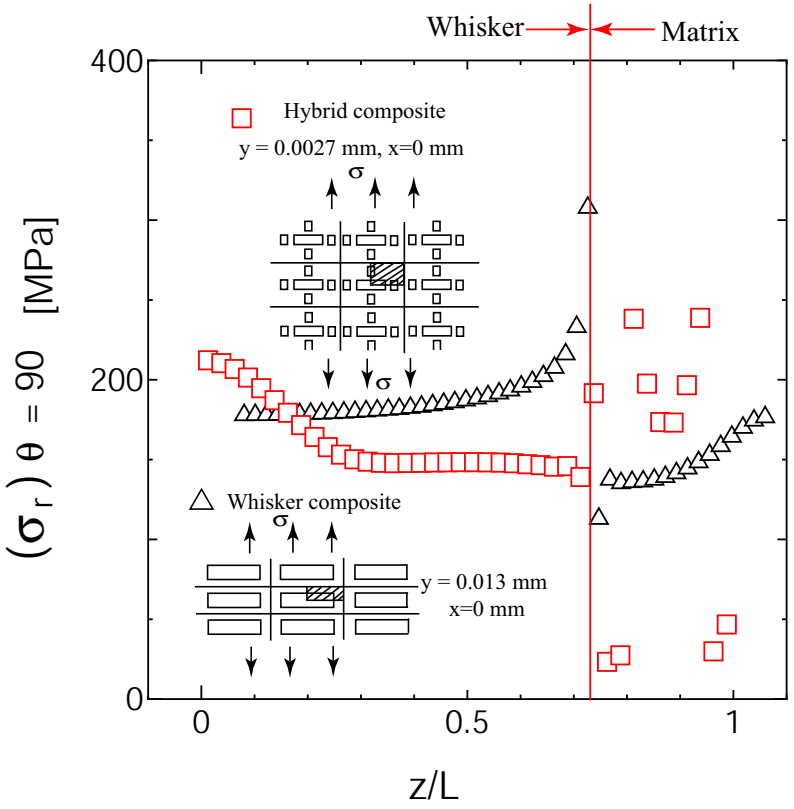

Fig. Stress distribution along direction for longitudinal loading (parallel to the stress direction)

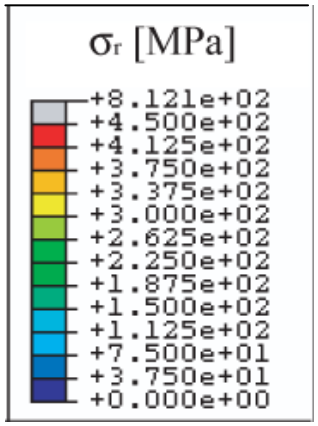

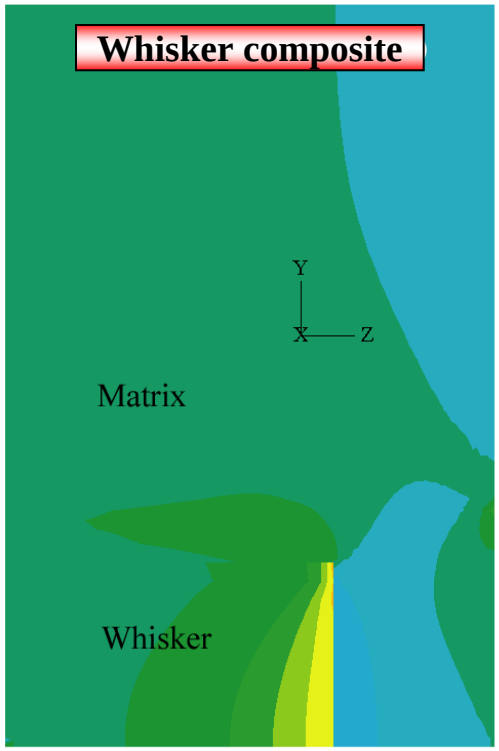

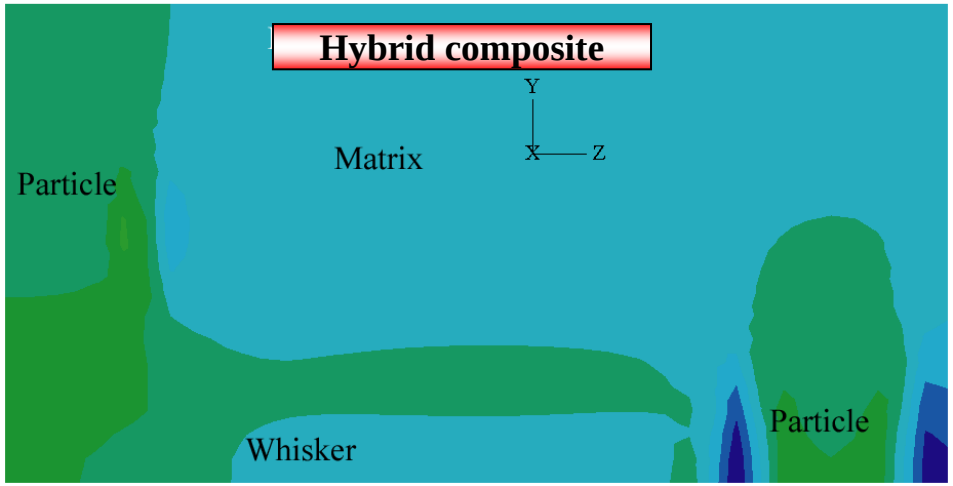

3.3.2 Numerical results and discussion

Others research
(Z. Trojanova et.all, 2005)

Whisker composite
25 % higher

Hybrid composite
16 % higher

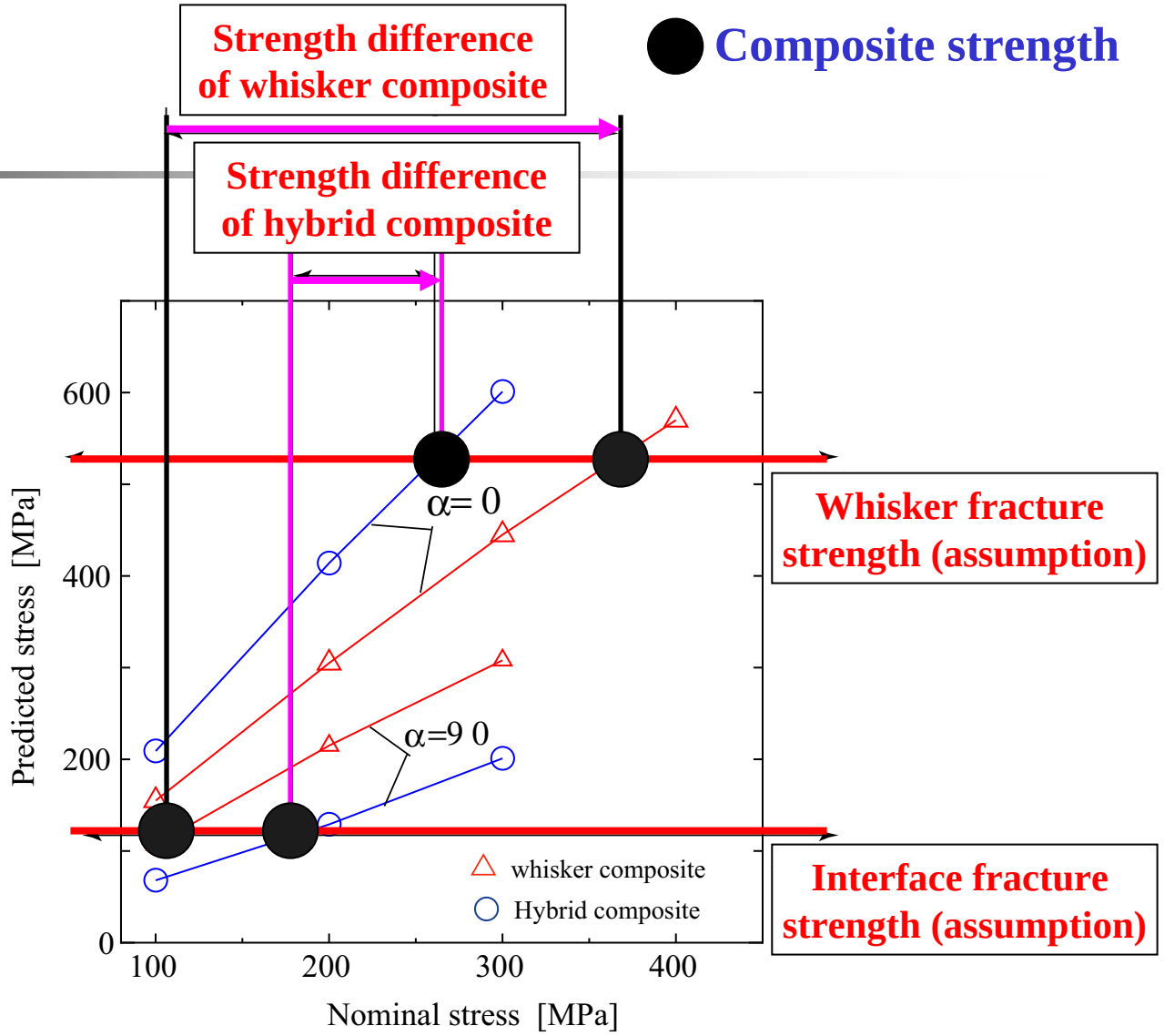

Fig. Predicted stress calculated from different nominal stress

3.3.3. Summary of numerical analysis

- **A three dimensional single whisker unit cell model in the periodic boundary condition is conducted.**
- **The maximum stress site is in the whisker when** $\alpha = 0^\circ$
- **High stress takes place in the interface between whisker and matrix when** $\alpha = 90^\circ$
- **Whisker orientation effect on hybrid composite is lower than the whisker composite.**

4. Conclusions of our research

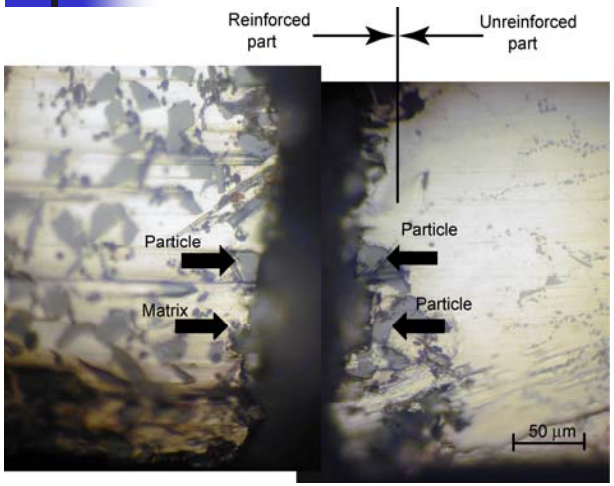

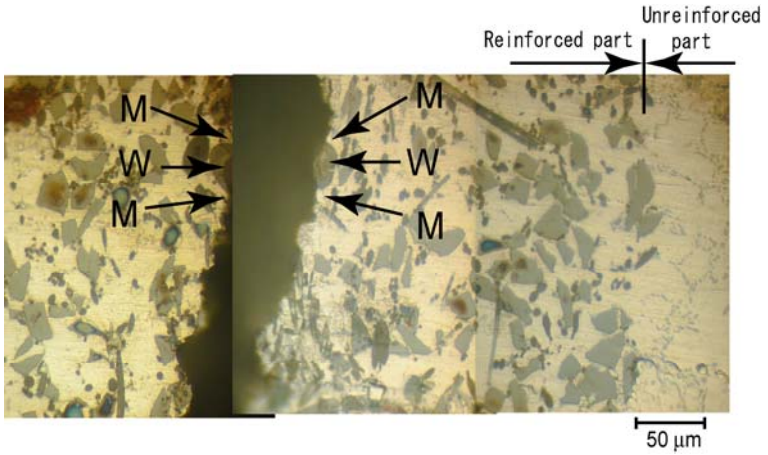

- **The fracture occurs in the reinforced part under both monotonic and cyclic load**

4. Conclusions of our research

Load type	SiC particle		Al_2O_3 whisker	
	F, %	D, %	F, %	D, %
Monotonic	10.5	10.1	0.85	9.3
Cyclic	1.9	19.0	0.85	8.9

F is fracture area and D is debonding area

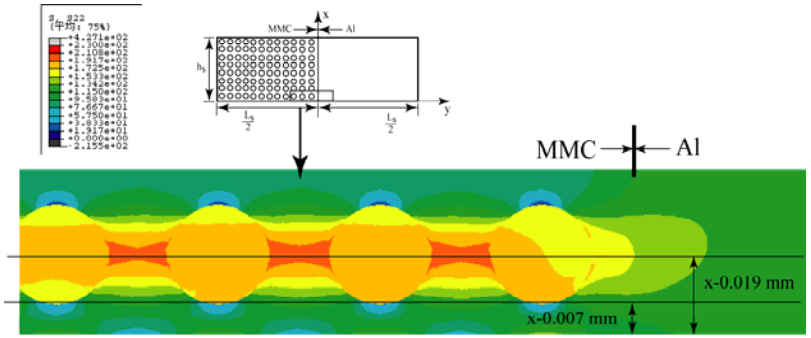

- **Under cyclic load, the fracture is dominated by interfacial debonding of particle/matrix and whisker/matrix interface**

4. Conclusions of our research

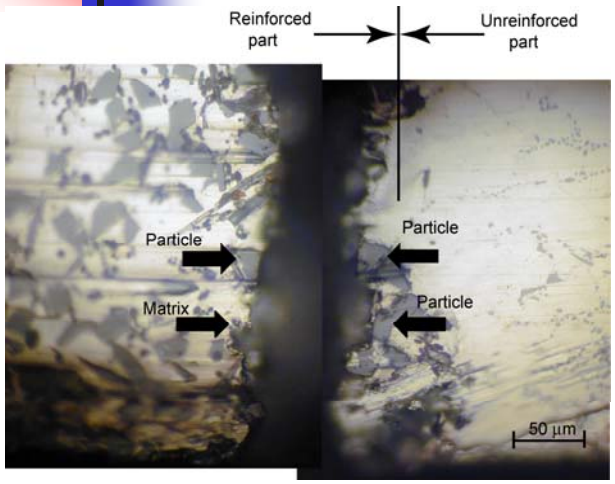

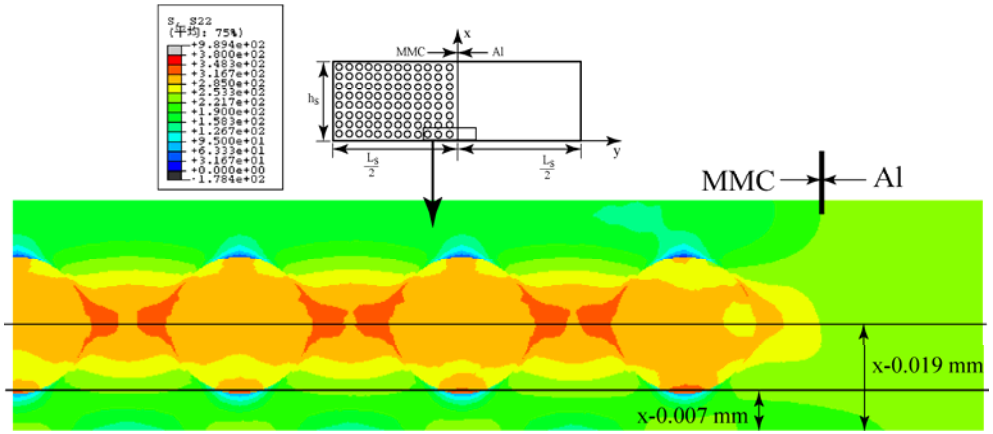

- **Under monotonic load, fracture occurs at the particle closest to the unreinforced part.**

4. Conclusions of our research

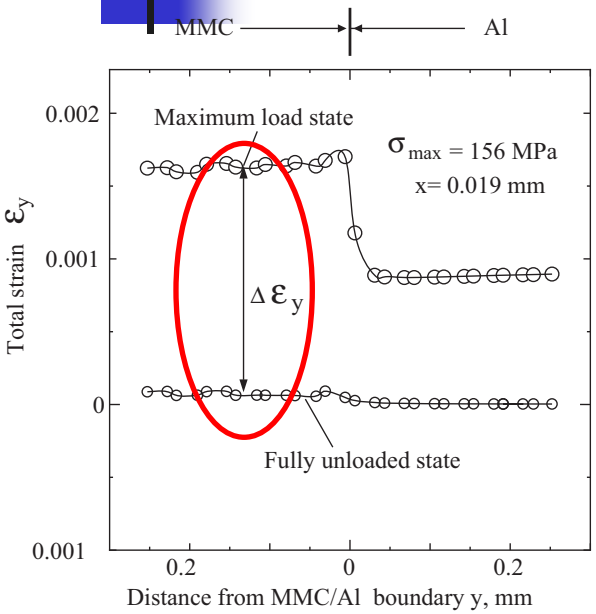

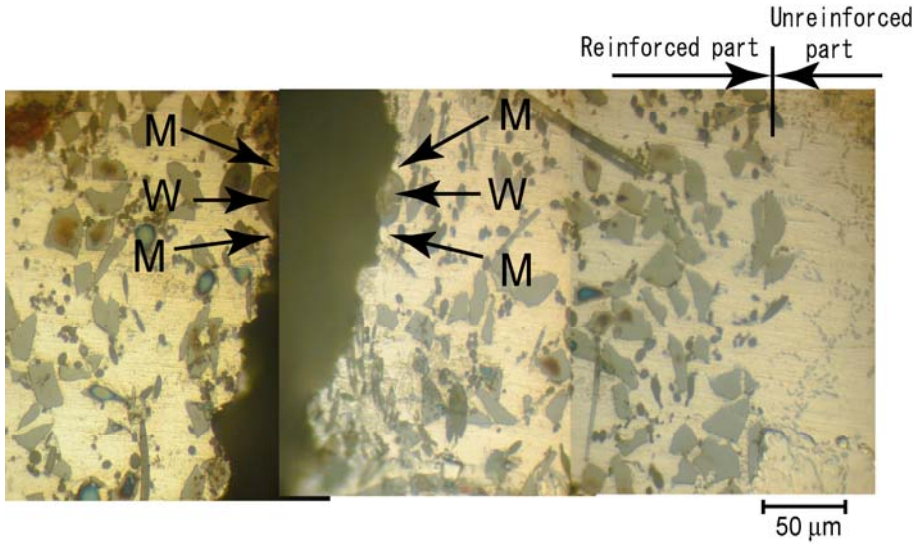

- **As for the fatigue analysis, the predicted strain amplitude in the matrix during cyclic loading is much higher in the reinforced part compared to the unreinforced part.**

4. Conclusions of our research

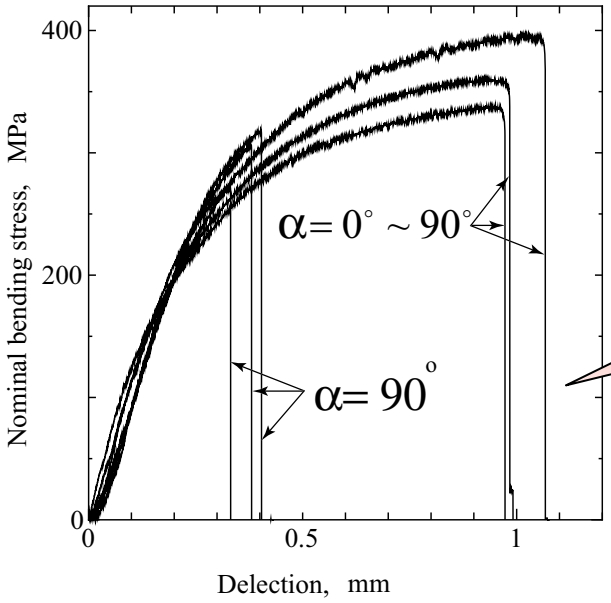

Fig. Nominal bending stress versus deflection curves under monotonic loading.

(Our research)

18% higher strength for parallel orientation

$\alpha = 0^\circ \sim 90^\circ$

(Others research)

(Z. Trojanova et.all, 2005)

16% higher strength for parallel orientation $\alpha = 0^\circ$

4. Conclusions of our research

Material	SiC particle		Al_2O_3 whisker	
	F, %	D, %	F, %	D, %
α=90°	1.2	19.6	0.6	9.1
α=0° – 90°	1.9	20.6	11	0.1

F is fracture area and D is debonding area

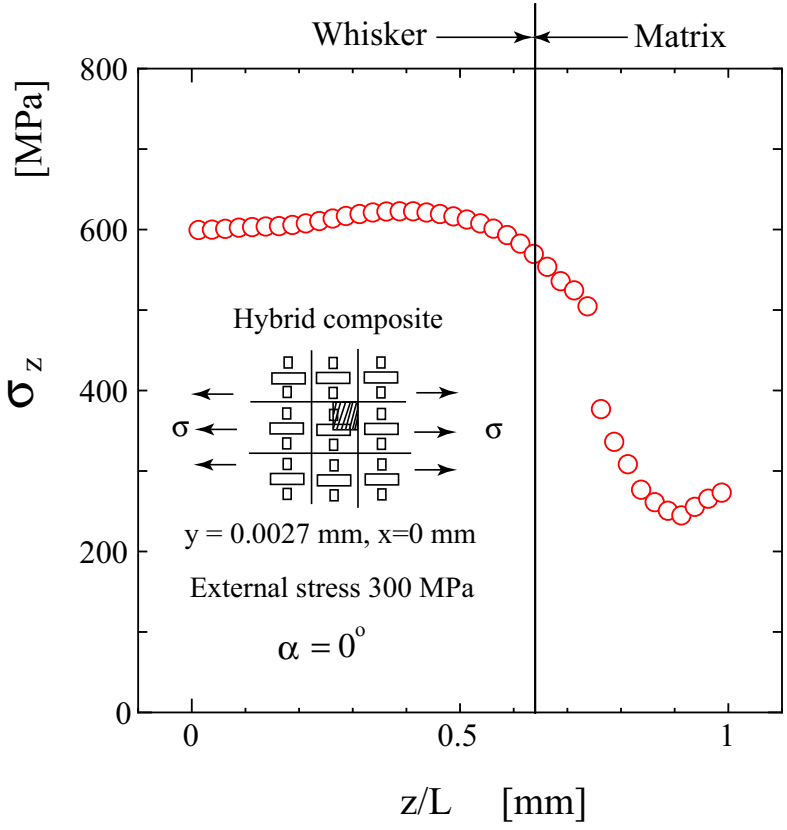

4. Conclusions of our research

Material	SiC particle		Al_2O_3 whisker	
	F, %	D, %	F, %	D, %
α=90°	1.2	19.6	0.6	9.1
α=0° – 90°	1.9	20.6	11	0.1

F is fracture area and D is debonding area

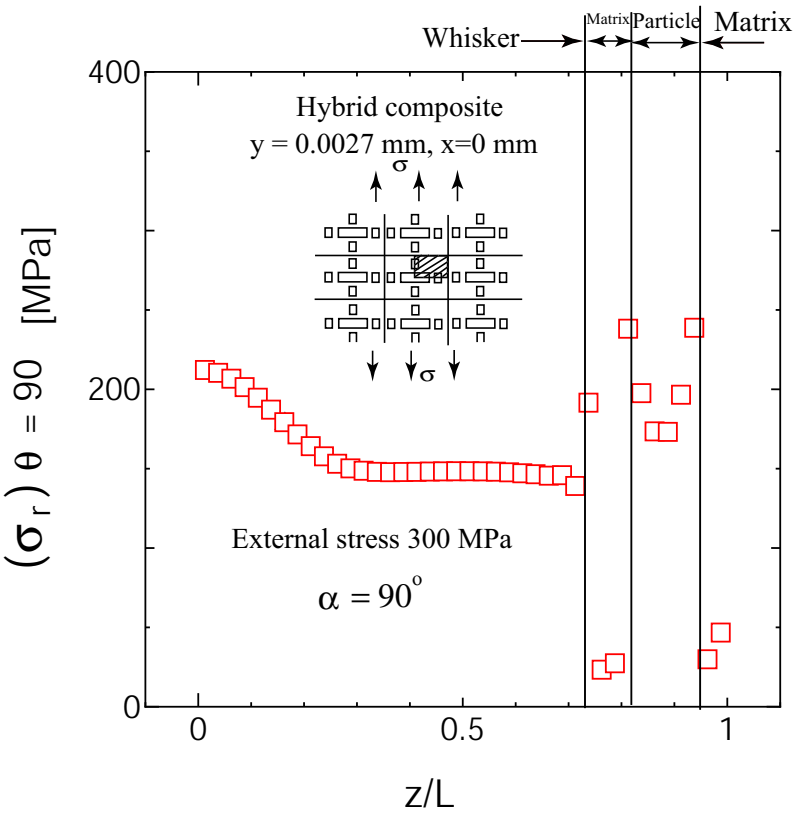

4. Conclusions of our research

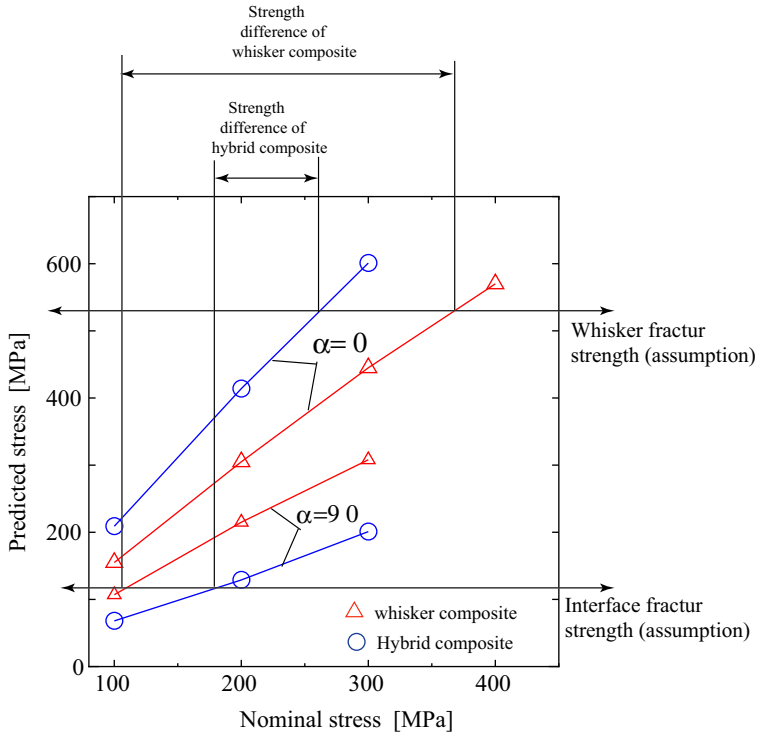

➢ **whisker orientation effect on hybrid composite is lower than the whisker composite.**

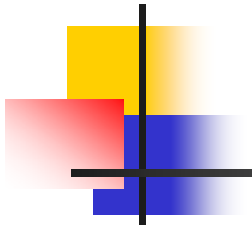

Thank You!